A&A 475, 19–36 (2007)
DOI: 10.1051/0004-6361:20065366

Astronomy & Astrophysics

The Weibel instability in relativistic plasmas

II. Nonlinear theory and stabilization mechanism

A. Achterberg[1], J. Wiersma[1], and C. A. Norman[1,2]

[1] Sterrenkundig Instituut, Universiteit Utrecht, PO Box 80000, 3508 TA Utrecht, The Netherlands
e-mail: a.achterberg@astro.uu.nl
[2] Dept. of Physics and Astronomy, Johns Hopkins University, Homewood Campus, Baltimore MD 21218, USA

Received 5 April 2006 / Accepted 9 August 2007

ABSTRACT

Aims. We discuss the onset of the nonlinear stage of the electromagnetic Weibel instability in a relativistic plasma, and the process of current coalescence that follows this instability. The Weibel instability has been proposed as a possible source of the magnetic fields needed to explain the non-thermal synchrotron emission from gamma ray bursts.
Methods. We present two different calculations of the nonlinear saturation of the Weibel instability: one based on a fluid model, and one using kinetic plasma theory. These approaches yield a similar result for the amplitude of the magnetic field at saturation. We then consider the further growth of the magnetic field due to the coalescence of current filaments, a process that has been observed in numerical simulations.
Results. These calculations show that the exponential linear stage of the instability is terminated by trapping of the beam particles in the wave. The trapping leaves a magnetic field that acts as the seed field for further amplification through coalescence. Further field amplification is limited to magnetic fields on scales less than the effective plasma skin depth of a background plasma. We show that coalescence of current filaments thicker than a few times the skin depth proceeds at a exponentially slow rate.
Conclusions. The amplitude of saturation is determined mostly by the plasma frequency of the hot (shocked) background plasma, which is usually dominated by the electrons. The typical field amplitude at this stage is almost independent of the mass of the beam particles. Further field amplification through current coalescence, a process that follows the exponential Weibel instability, "stalls" once the current filaments reach a size that is comparable to the skin depth of the background plasma. This process concentrates the currents, but the resulting field amplification is small. This implies that the resulting magnetic field energy density never reaches equipartition with the kinetic energy density of the heavy particle species (ions) in the incoming beams.

Key words. plasmas – magnetic fields – instabilities – shock waves – galaxies: jets – gamma rays: bursts

1. Introduction

The Weibel instability is a plasma instability that arises in plasmas with an anisotropic velocity distribution. This article discusses the nonlinear dynamics of the plasma in the late stages of this instability in the relativistic shock fronts that are produced by gamma ray burst sources. In this situation, the Weibel instability is beam-driven, and is sometimes referred to as the *filamentation instability*.

The prompt and afterglow emission from gamma ray bursts (GRBs) is often interpreted as synchrotron emission or as jitter radiation (Medvedev 2000) from relativistic electrons in a magnetic field. In order to explain the intensity of the observed radiation, the magnetic field in the emission region must have a strength of 1 to 10% of the equipartition field strength B_e, e.g. Wijers & Galama (1999), which is defined in terms of the internal (thermal) energy e of the plasma as

$$B_e = \sqrt{8\pi e}. \quad (1)$$

This holds true for both the emission from internal shocks (see Rees & Mészáros 1994), which are believed to be responsible for the prompt emission, and for the emission from external shocks (e.g. Rees & Mészáros 1992) which are believed to be the source of the afterglow emission. A full account of the observations and theory of GRBs can be found in the reviews of Piran (2000, 2004) and of Mészáros (2002, 2006).

The strong magnetic fields associated with GRBs must somehow be self-generated by the strong (relativistic) shocks invoked in those GRB models where most of the energy is in particles, as opposed to electromagnetic (Pointing flux dominated) models. In particular for the external shocks of GRBs that precede the fireball in the interstellar or circumstellar medium it can be shown that the compression of the pre-shock (interstellar/circumstellar) magnetic fields in a relativistic shock leads to $B \ll B_e$ in the post-shock plasma.

It has been proposed, see Medvedev & Loeb (1999) and Gruzinov (2001), that the Weibel instability leads to the generation of the necessary magnetic fields. The basic picture is that this instability operates in the shock transition layer, where the unshocked incoming plasma mixes with the (relativistically) hot shocked plasma. The mixture is unstable against the generation of low-frequency electromagnetic waves with $|\omega| \ll kc$, where ω is the wave frequency and $k = 2\pi/\lambda$ is the wave number. This instability is due to the anisotropy of the momentum distribution of the incoming plasma, which looks like a beam in the reference frame of the shocked plasma. Since Maxwell's equations imply that the Fourier amplitudes $\tilde{\boldsymbol{E}}$ and $\tilde{\boldsymbol{B}}$ of the electric and magnetic fields associated with the instability satisfy the

relation $|\tilde{\boldsymbol{E}}| \sim (|\omega|/kc)\,|\tilde{\boldsymbol{B}}| \ll |\tilde{\boldsymbol{B}}|$, the resulting turbulent electromagnetic field is almost purely magnetic.

Although it is now long known that the Weibel instability can generate magnetic fields in relativistic shock fronts, estimates of the attainable magnetic field strength have been mostly restricted to ad hoc arguments. In this article we present an in-depth look into the nonlinear dynamics of a Weibel-unstable plasma to obtain a reliable foundation for our estimates of the attainable magnetic field strength. In addition, we discuss the mechanisms that contribute to the stabilization of the Weibel instability and the subsequent thermalization of the plasma.

Our calculations concentrate on the case of ultra-relativistic shocks, with a bulk Lorentz factor of the incoming flow $\gamma \gg 1$. We will assume that we can model the plasma in the shock front with two symmetric counterstreaming plasmas because the effect of asymmetries is small (Achterberg & Wiersma 2007). We also take the beams to be cold, as one would expect in a shock front encountering the cold interstellar medium. At various points, we will take into account the presence of a relativistically hot and stationary background plasma that corresponds to the already thermalized post-shock plasma. We discuss the kinetic and fluid processes that take place on time and length scales in the order of the plasma frequency and plasma skin depth, respectively.

In the companion paper Achterberg & Wiersma (2007) (from this point on: AW1) we have considered the linear phase of the Weibel instability, where the magnetic field grows exponentially in time. In this paper we consider the case where the unperturbed plasma is unmagnetized. As shown in AW1, Sect. 8, the effects of a pre-existing ambient magnetic field on the growth of the Weibel instability is small for the typical parameters associated with gamma ray bursts. The main conclusions of AW1 can be summarized as follows:

The growth rate of the instability due to two equal but counterstreaming beams in the presence of a (hot) background plasma is mostly determined by two parameters: η and $\mathcal{M}$. The first parameter is defined as

$$\eta = \left(\hat{\omega}_{\rm pb}/\tilde{\omega}_{\rm bg}\right)^2, \tag{2}$$

the square of the ratio of the effective plasma frequency $\hat{\omega}_{\rm pb}$ of the beam particles and the the plasma frequency $\tilde{\omega}_{\rm bg}$ of thermal background. In a hydrogen plasma, the background plasma frequency is almost entirely determined by the contribution of the hot electrons and one has

$$\tilde{\omega}_{\rm bg}^2 \simeq \frac{4\pi e^2 n_{\rm e}}{m_{\rm e} h_{\rm e}}. \tag{3}$$

Here $h_{\rm e}$ is the enthalpy per unit rest energy of the electron gas, with $h_{\rm e} \approx 1$ if the electron gas is cold so that $k_{\rm b}T_{\rm e} \ll m_{\rm e}c^2$, and $h_{\rm e} \simeq k_{\rm b}T_{\rm e}/m_{\rm e}c^2 \gg 1$ for a relativistically hot electron gas. The beam plasma frequency is

$$\hat{\omega}_{\rm pb}^2 = \frac{4\pi q_{\rm b}^2 n_{\rm b}}{m_{\rm b} h_{\rm b}}, \tag{4}$$

in terms of the charge $q_{\rm b}$ and mass $m_{\rm b}$ of the beam particles, their proper density $n_{\rm b}$ and the enthalpy per unit rest energy $h_{\rm b}$. When the beams are cold we have $h_{\rm b} \simeq 1$.

The parameter $\mathcal{M}$ can be thought of as an effective "beam Mach Number": it is a measure for the importance of the velocity dispersion in the beam plasma in the direction perpendicular to the beam direction, which we will take along the z-axis. If the magnitude of the momentum of the directed motion of the beam particles is p_{z0} and if the typical momentum associated with the velocity dispersion perpendicular to the beam direction is p_{x0}, one has:

$$\mathcal{M} \sim p_{z0}/p_{x0}. \tag{5}$$

A full set of definitions can be found in AW1, Sects. 5 and 6, where both a fully relativistic fluid model and a waterbag model employing kinetic theory are employed to describe the beams. If the beams are infinitly cold one has $\mathcal{M} \to \infty$. As we will see below, the value of $\mathcal{M}$ together with η determines the range of unstable wave numbers, and η determines the maximum growth rate.

In the symmetric case, where the beam particles are distributed over two counterstreaming but otherwise identical beams, each with proper density $n_{\rm b}/2$, there is a simple approximation for the growth rate of the instability in the limit of perturbations with the wavevector perpendicular to the beam direction: $\boldsymbol{k} \cdot \boldsymbol{V}_{\rm b} = 0$. This approximation is almost universally valid for ultra-relativistic beams (with $p_{z0} \gg m_{\rm b}c$) if $\mathcal{M} \gg 1$, $\eta \leq 1$ and $\eta\mathcal{M}^2 \gg 1$, and still gives rather good approximation for $\eta \sim \mathcal{M} \sim 1$. In terms of a dimensionless growth rate and wave number, defined as

$$\sigma \equiv {\rm Im}(\omega)/\tilde{\omega}_{\rm bg} \quad , \quad \kappa \equiv kc/\tilde{\omega}_{\rm bg}, \tag{6}$$

one finds:

$$\sigma^2(\kappa) \approx \frac{\kappa^2}{\kappa_{\rm s}^2 + \kappa^2}\left(\frac{\kappa_{\rm max}^2 - \kappa^2}{\mathcal{M}^2}\right). \tag{7}$$

Here $\kappa_{\rm s}$ is the (dimensionless) wave number below which screening currents in the background plasma slow the growth of the instability, see AW1[1], Sect. 6 (Eq. (46)) and Sect. 7 (Eqs. (57) and (60)). In our application to ultra-relativistic beams one has $\kappa_{\rm s} \sim 0.1$–1.

The wave number $\kappa_{\rm max}$ is the maximum unstable wave number that, in the limit $\eta\mathcal{M}^2 \gg 1$ that concerns us here, equals

$$\kappa_{\rm max} \equiv \sqrt{\eta\mathcal{M}^2 - 1} \approx \sqrt{\eta}\,\mathcal{M}. \tag{8}$$

The maximum growth rate, which follows from ${\rm d}\sigma/{\rm d}\kappa = 0$, occurs at a wave number κ_*, which for dispersion relation (7) is given by

$$\kappa_* = \left(\kappa_{\rm s}\,\sqrt{\kappa_{\rm max}^2 + \kappa_{\rm s}^2} - \kappa_{\rm s}^2\right)^{1/2} \approx \sqrt{\kappa_{\rm s}\kappa_{\rm max}}. \tag{9}$$

It equals $\sigma(\kappa_*) \equiv \sigma_*$, which is:

$$\sigma_* = \frac{\sqrt{\kappa_{\rm s}^2 + \kappa_{\rm max}^2} - \kappa_{\rm s}}{\mathcal{M}} \approx \frac{\kappa_{\rm max}}{\mathcal{M}} = \sqrt{\eta}. \tag{10}$$

In these two expressions the last approximate terms on the right-hand side are valid in the limit $\eta\mathcal{M}^2 \gg 1$, when $\kappa_{\rm max} \gg \kappa_{\rm s}$.

This implies that the Weibel instability is most vigorous at wavelengths shorter than the effective skin depth $\lambda_{\rm sk} \sim c/\tilde{\omega}_{\rm bg}\kappa_{\rm s}$ of the hot background plasma. The linear growth rate is almost independent of wave number, and close to σ_*, on a broad "plateau" in the wave number range corresponding

[1] Note that in this paper we write k (rather than K as in AW1): for the wave number in the laboratory frame, which coincides with the rest frame of the thermal plasma.

to $\kappa_s < \kappa < \kappa_{max}$, see Figs. 1 and 2 of AW1. The maximum unstable wavelength is determined by the "temperature" of the beam plasma, which determines the value of $\mathcal{M}$ through the velocity dispersion of beam particles along the wave vector.

In the rest of this article we will discuss the stabilization of the Weibel instability and the subsequent evolution of the plasma. In Sect. 2 we start of with an overview of stabilisation mechanisms that have already been discussed in the literature. In Sect. 3 we present a fluid model for the nonlinear wave breaking of a single wave mode of the Weibel instability. In Sect. 4 we briefly consider a kinetic model for the nonlinear dynamics of the Weibel-unstable plasma once a broad-band spectrum of unstable modes has been excited. In Sect. 5 we estimate whether and for how long the electrical currents can keep growing stronger after the instability itself has stabilized. Section 6 discusses the implications of our results for the plasma in an ultra-relativistic shock front, considering thermalization of the electrons and the ions in the plasma separately. For the ions we estimate the thermalization length scale due to scattering in the turbulent magnetic fields produced by the Weibel instability. In Sect. 7 we summarize the conclusions that we draw from our results.

2. Stabilization mechanisms: an overview

A number of stabilization mechanisms have been proposed for the beam-driven Weibel instability in an astrophysical context. In this section we compare two mechanisms employed in recent literature to estimate the attainable magnetic field strength of the Weibel instability: magnetization of the beam particles and magnetic trapping of particles in the wave fields. We will show that the latter gives the most stringent limit on the attainable magnetic field amplitude for the parameter regime that we are interested in.

Medvedev & Loeb (1999) have proposed that the deflection of beam particles in the self-generated magnetic field stabilizes the instability when the Larmor radius in this field becomes of the order of the wavelength of the most unstable mode. This essentially means that the beam particles become magnetized. For simplicity we consider the case of a cold beam.

The gyration radius r_g of beam particles of mass m_b, beam velocity V_b, bulk (beam) Lorentz factor $\gamma_b = 1/\sqrt{1 - V_b^2/c^2}$ and charge q_b is of order:

$$r_g = \frac{\gamma_b m_b c V_b}{q_b B} = \frac{V_b}{\Omega_g}. \tag{11}$$

Here $\Omega_g = q_b B/\gamma_b m_b c$ is the gyration frequency of the beam particles in a magnetic field of strength B. The corresponding stabilization criterion according to Medvedev & Loeb (1999) reads:

$$k_* r_g = \frac{k_* V_b}{\Omega_g} \sim 1, \tag{12}$$

with k_* the wave number of the fastest growing mode. We will refer to this as the *magnetization criterion*.

Alternatively, Yang et al. (1994) have proposed that magnetic trapping of particles in the waves stabilizes the Weibel instability. This stabilization mechanism was already considered by Davidson et al. (1972) for the non-relativistic Weibel instability in a plasma with a temperature anisotropy. The same stabilization mechanism was briefly discussed by Gruzinov (2001) in the context of magnetic field generation in GRB shocks.

The electromagnetic field of the waves produced by the instability will cause the beam particles to "quiver". Trapping occurs when the amplitude of the quiver motion in the direction of the wave vector reaches an amplitude comparable to the wavelength of the unstable mode. This quiver motion is induced by the Lorentz force on the beam particles due to the wave magnetic field $\boldsymbol{B} = B(x\,,\,t)\,\hat{\boldsymbol{y}}$. The equation of motion to first order in the wave amplitude reads (see also the more complete treatment below)

$$\frac{\mathrm{d}^2\xi_x}{\mathrm{d}t^2} = -\frac{q_b V_b B}{\gamma_b m_b c}, \tag{13}$$

with ξ_x the displacement of a beam particle in the x-direction. For a magnetic field varying as $B(x\,,\,t) = B_0 \exp(\tilde{\sigma} t)\,\sin(kx)$, with $\tilde{\sigma} = \mathrm{Im}(\omega) > 0$ the growth rate of the instability, one finds that the typical amplitude of the quiver motion is

$$|\xi_x| \approx \left|\frac{q_b V_b B}{\gamma_b m_b c \tilde{\sigma}^2}\right|. \tag{14}$$

The stabilization condition reads (e.g. Davidson 1972)

$$|k\,\xi_x| = \left|k\,\frac{q_b V_b B}{\gamma_b m_b c \tilde{\sigma}^2}\right| \sim 1, \tag{15}$$

which we will refer to as the *trapping criterion*.

As was pointed out in Wiersma & Achterberg (2004), the trapping criterion (15) is the most stringent criterion of the two for external GRB shocks, which have $\eta \le 1$, $V_b \simeq c$ and $\mathcal{M} \gg 1$. This is easily checked for dispersion relation (7). From (12) and (15) one finds that the field amplitudes B^m and B^{tr} predicted respectively by these two criteria are:

$$B^m \sim \frac{\gamma_b m_b c\, k_* V_b}{q_b} \quad , \quad B^{tr} \sim \frac{\gamma_b m_b c\, \tilde{\sigma}^2(k_\dagger)}{q_b k_\dagger V_b}. \tag{16}$$

Here $k_\dagger$ is the wave number where $\tilde{\sigma}^2(k)/k$ reaches its maximum value. We define a third characteristic dimensionless parameter,

$$\alpha \equiv \sqrt{1 + \frac{\kappa_{max}^2}{\kappa_s^2}}\,, \tag{17}$$

with the beam-driven Weibel instability occurring for $\alpha > 1$. The characteristic dimensionless wave numbers $\kappa_* = k_* c/\tilde{\omega}_{bg}$, $\kappa_\dagger = k_\dagger c/\tilde{\omega}_{bg}$ and $\kappa_{max} = k_{max} c/\tilde{\omega}_{bg}$ can be written in terms of α as

$$\kappa_{max} = \kappa_s\,\sqrt{\alpha^2 - 1}\ \ ,\ \ \kappa_* = \kappa_s\,\sqrt{\alpha - 1}\ \ ,\ \ \kappa_\dagger = \kappa_s\,S(\alpha), \tag{18}$$

with $S(\alpha)$ for dispersion relation (7) given by:

$$S(\alpha) \equiv \left\{\frac{\alpha}{2}\,\sqrt{8 + \alpha^2} - 1 - \frac{\alpha^2}{2}\right\}^{1/2}. \tag{19}$$

The ratio of the field amplitudes B^{tr} and B^m can be written for $V_b \simeq c$ as

$$\frac{B^{tr}}{B^m} = \frac{\sigma_\dagger^2}{\kappa_\dagger \kappa_*} = \frac{S(\alpha)}{\sqrt{\alpha - 1}\,\mathcal{M}^2}\left(\frac{3\alpha - \sqrt{8 + \alpha^2}}{\sqrt{8 + \alpha^2} - \alpha}\right), \tag{20}$$

where $\sigma_\dagger = \tilde{\sigma}(k_\dagger)/\tilde{\omega}_{bg}$. For $\alpha \gg 1$ ($\eta\mathcal{M}^2 \gg 1$) one has $\kappa_{max} \simeq \alpha\kappa_s = \sqrt{\eta}\mathcal{M}$, $\kappa_* \simeq \sqrt{\alpha}\kappa_s$, $\kappa_\dagger \simeq \kappa_s$ and $\sigma_\dagger \simeq \kappa^{max}/\sqrt{2}\mathcal{M} = \sqrt{\eta/2}$.

In that case (20) reduces to

$$\frac{B^{\rm tr}}{B^{\rm m}} \simeq \frac{\eta}{2\sqrt{\alpha}\kappa_{\rm s}^2} = \frac{\eta^{3/4}}{2\kappa_{\rm s}^{3/2}\mathcal{M}^{1/2}}. \tag{21}$$

For GRB external shocks, with $\eta \leq 1$, $\alpha \gg 1$, $\mathcal{M} \gg 1$ and $\kappa_{\rm s} \leq 1$ one has $B^{\rm tr} \ll B^{\rm m}$, and trapping rather than magnetization stabilizes the beam-driven Weibel instability.

For the Weibel instability operating in the transition layer of an ultra-relativistic shock one expects $\eta \approx 1$ for an electron(-positron) beam, and $\eta \approx 4m_{\rm e}/3m_{\rm p} \simeq 7 \times 10^{-4}$ for a proton beam in a hot electron background, see Wiersma & Achterberg (2004) for more details. Since one must have $\mathcal{M} > 1 + 1/\eta$ for an instability to occur this implies that trapping will occur long before the beam particles are fully magnetized so that the exponential growth of the magnetic field saturates at $|B| \simeq B^{\rm tr}$.

Figure 1 shows the characteristic wave numbers κ_* and $\kappa_\dagger$ and $\kappa_{\rm max}$, and the ratio of the field amplitudes at trapping and magnetization, $B^{\rm tr}/B^{\rm m} = \sigma_\dagger^2/\kappa_\dagger\kappa_*$, all as a function of the parameter α for $\mathcal{M} = 100$.

3. Nonlinear effects: fluid model for the beam response

We now present detailed calculations that justify the order-of-magnitude estimates of the previous section for two different situations. In this section we consider the nonlinear effects due to the Weibel instability using a fluid model. This allows us to investigate the effect of nonlinear coupling, and in particular of *wave breaking* of the Weibel mode when only a single dominant mode of given wave number k is present. In the next section we will consider the kinetic theory, which is appropriate for a broad-band spectrum of unstable modes with bandwidth $\Delta k \sim k$, and where *phase mixing* of the quiver motion in the collection of waves is the dominant stabilization process. Since wave breaking generates higher harmonics (see below), the single-mode case will evolve naturally into the case of a broad-band spectrum.

For stable plasma modes (with a real frequency ω) a fluid calculation such as presented below would yield the well-known equations for *mode coupling* in the fluid approximation, see for instance Galeev & Sagdeev (1979). This coupling leads to resonant interactions between different waves (normal modes) of the form $\boldsymbol{k}_1 \pm \boldsymbol{k}_2 = \boldsymbol{k}_3$, $\omega_1 \pm \omega_2 = \omega_3$, where the indices enumerate the different wave modes. However, in the case of the unstable Weibel modes considered here such resonances do not occur as ω is purely imaginary. The dominant effect is through the nonlinear distortion of the wave profile, not unlike what happens to large-amplitude electron plasma oscillations in a cold plasma, see Davidson (1972), Ch. 3. This is a non-resonant process.

In order to keep the mathematics tractable we make a number of simplifying assumptions:

1. We treat the symmetric case with two oppositely directed beams of equal strength propagating along the z-axis with velocity $\boldsymbol{V}_\pm = \pm V_{\rm b}\,\hat{\boldsymbol{z}}$. In that case the *linear* Weibel mode is purely electromagnetic. We also assume that all electromagnetic fields vary as plane waves in the x-direction ($\boldsymbol{k} = k\,\hat{\boldsymbol{x}}$), so that $E(x\,,\,t)$, $B(x\,,\,t) \propto \exp(ikx - i\omega t)$. The Fourier amplitudes $\tilde{\boldsymbol{B}}$ and $\tilde{\boldsymbol{E}}_\perp$ of the electromagnetic field then satisfy
$$\tilde{\boldsymbol{B}} = \tilde{B}(k\,,\,\omega)\,\hat{\boldsymbol{y}} \;\;,\;\; \tilde{\boldsymbol{E}}_\perp = \tilde{E}_\perp(k\,,\,\omega)\,\hat{\boldsymbol{z}} = -\frac{\omega}{kc}\,\tilde{B}(k\,,\,\omega)\,\hat{\boldsymbol{z}}. \tag{22}$$
The last relation follows from Faraday's law: $c(\boldsymbol{\nabla}\times\boldsymbol{E}) + \partial\boldsymbol{B}/\partial t = 0$. Here we use the subscript $\perp$ to distinguish the transverse electric field (with $\boldsymbol{k}\cdot\tilde{\boldsymbol{E}}_\perp = 0$) from the longitudinal electric field $\tilde{\boldsymbol{E}}_\parallel = \tilde{E}_\parallel(k\,,\,\omega)\,\hat{\boldsymbol{x}}$ that is introduced below.
2. We consider the wavelength range where $|\omega|/kc \ll 1$. For the low-frequency electromagnetic Weibel mode this implies that the magnetic field amplitude is much larger than the amplitude of the transverse electric field:
$$\left|\tilde{B}(k\,,\,\omega)\right| = \left|\frac{kc}{\omega}\right|\,\left|\tilde{E}_\perp(k\,,\,\omega)\right| \gg \left|\tilde{E}_\perp(k\,,\,\omega)\right|.$$
3. For the moment we will neglect pressure effects in the beam dynamics, putting the kinetic temperature of the beam particles equal to zero.

In this case, the equation of motion for the fluid of beam particles is formally the same as that for a *single* particle of mass $m_{\rm b}$ and charge $q_{\rm b}$:

$$\frac{{\rm d}\boldsymbol{p}}{{\rm d}t} = q_{\rm b}\left(\boldsymbol{E} + \frac{\boldsymbol{V}\times\boldsymbol{B}}{c}\right). \tag{23}$$

Here $\boldsymbol{p}(\boldsymbol{x}\,,\,t)$ is the momentum of the fluid, defined as usual in terms of the fluid velocity $\boldsymbol{V}(\boldsymbol{x}\,,\,t)$ as

$$\boldsymbol{p} = \gamma m_{\rm b}\boldsymbol{V} = \frac{m_{\rm b}\boldsymbol{V}}{\sqrt{1 - V^2/c^2}}. \tag{24}$$

The time-derivative in Eq. (23) should be interpreted as the convective (Lagrangian) time derivative,

$$\frac{\rm d}{{\rm d}t} \equiv \frac{\partial}{\partial t} + \boldsymbol{V}\cdot\boldsymbol{\nabla}. \tag{25}$$

We consider the symmetric case with two counterstreaming but otherwise identical beams, directed along the z-axis. Each beam has an unperturbed laboratory frame density $n_+ = n_- = \overline{n}_{\rm b}/2$. Here, and in what follows, we use a subscript $\pm$ to distinguish quantities associated with the forward beam (with unperturbed velocity $\boldsymbol{V} = +V_{\rm b}\,\hat{\boldsymbol{z}}$) and the backward beam (with unperturbed velocity $\boldsymbol{V} = -V_{\rm b}\,\hat{\boldsymbol{z}}$) . The density of these two beams satisfies the continuity equation,

$$\frac{\partial n_\pm}{\partial t} + \boldsymbol{\nabla}\cdot(n_\pm\boldsymbol{V}_\pm) = 0. \tag{26}$$

Note that the *proper* density of each of the two beams is $n_{0\pm} = n_\pm/\gamma_\pm$, with $\gamma_\pm = 1/\sqrt{1 - |\boldsymbol{V}_\pm|^2/c^2}$. Finally, the charge density and current density associated with the two beams is

$$\rho_\pm = q_{\rm b}n_\pm \;\;,\;\; \boldsymbol{J}_\pm = q_{\rm b}n_\pm\,\boldsymbol{V}_\pm. \tag{27}$$

3.1. Dynamics of the beam particles

The equation of motion in the x and z direction reads respectively:

$$\left(\frac{\partial}{\partial t} + V_x\,\frac{\partial}{\partial x}\right)p_x \;=\; q_{\rm b}\left(E_\parallel - \frac{V_z}{c}B\right); \tag{28}$$

$$\left(\frac{\partial}{\partial t} + V_x\,\frac{\partial}{\partial x}\right)p_z \;=\; q_{\rm b}\left(E_\perp + \frac{V_x}{c}B\right). \tag{29}$$

The y-component reads ${\rm d}p_y/{\rm d}t = 0$, and we can put $p_y = 0$.

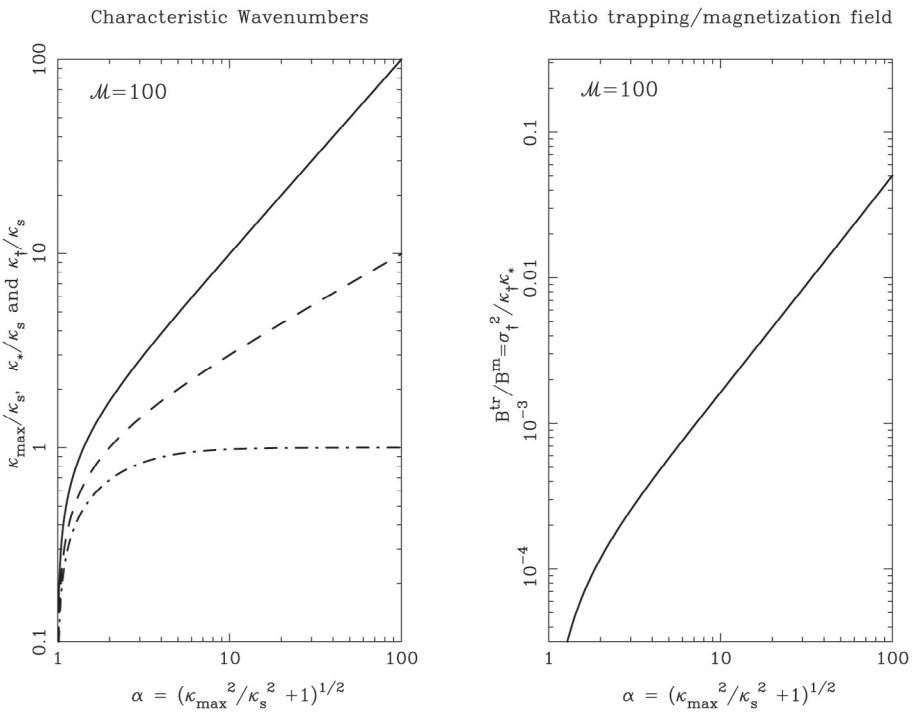

Fig. 1. *The lefthand panel* shows, as a function of α and for a beam Mach number $\mathcal{M} = 100$, the behavior of the maximum unstable wave number $\kappa_{\rm max}$ (solid curve), the wave number κ_* of the maximum linear growth rate (dashed curve), and the wave number $\kappa_\dagger$ associated with the largest wave amplitude in the case of stabilization by trapping (dash-dot curve). *The righthand panel* shows, again as a function of α, the ratio of the magnetic field strength predicted by the trapping argument and the magnetization argument, $B^{\rm tr}/B^{\rm m}$.

The transverse electromagnetic fields are associated with the Weibel mode, and can be written in terms of a vector potential $\boldsymbol{A} = A(x\,,\,t)\,\hat{\boldsymbol{z}}$:

$$E_\perp = -\frac{1}{c}\,\frac{\partial A}{\partial t}\quad,\quad B = -\frac{\partial A}{\partial x}\cdot \tag{30}$$

The longitudinal electric field can be derived from a scalar potential $\Phi(x\,,\,t)$:

$$E_\parallel = -\frac{\partial \Phi}{\partial x}\cdot \tag{31}$$

In the Weibel instability of two counterstreaming beams of equal density ($n_+ = n_-$) this longitudinal field is absent in the linear approximation, and can only be excited nonlinearly by the beams (See AW1, Sect. 2.3, and the discussion below).

If one substitutes these definitions into the z-component of the equation of motion (Eq. (29)) one finds that it can be written as

$$\left(\frac{\partial}{\partial t} + V_x\,\frac{\partial}{\partial x}\right)\left(p_z + \frac{q_{\rm b}}{c}\,A\right) = \frac{{\rm d}P_z}{{\rm d}t} = 0, \tag{32}$$

with $P_z \equiv p_z + \frac{q_{\rm b}}{c}A$ the z-component of the canonical momentum. This can immediately be integrated to

$$P_z = p_z + \frac{q_{\rm b}}{c}\,A = {\rm const.}, \tag{33}$$

the conservation of the canonical momentum in the z-direction, which arises as z is an ignorable coordinate. If one turns on the waves adiabatically, it follows that one must have

$$(P_z)_\pm = \pm m_{\rm b}\gamma_{\rm b}V_{\rm b}, \tag{34}$$

i.e. the canonical momentum in the z-direction equals the unperturbed beam momentum.

We expand all fields as plane waves by defining the Fourier amplitudes for the vector and scalar potentials:

$$\begin{pmatrix} A(x\,,\,t) \\ \\ \Phi(x\,,\,t) \end{pmatrix} = \int \frac{{\rm d}k\,{\rm d}\omega}{(2\pi)^2} \begin{pmatrix} \tilde{A}(k\,,\,\omega) \\ \\ \tilde{\Phi}(k\,,\,\omega) \end{pmatrix} \exp({\rm i}kx - {\rm i}\omega t). \tag{35}$$

Maxwell's equations imply that the Fourier components of the electric and magnetic field are

$$\tilde{E}_\perp = \frac{{\rm i}\omega}{c}\,\tilde{A}\quad,\quad \tilde{B} = -{\rm i}k\,\tilde{A}\quad,\quad \tilde{E}_\parallel = -{\rm i}k\,\tilde{\Phi}\,. \tag{36}$$

In addition, we will assume that the beams are ultra-relativistic, with $\gamma_{\rm b} \gg 1$.

It is easily checked that the motion induced by the low-frequency Weibel mode in an ultra-relativistic beam is almost one-dimensional, with the perturbed velocity directed along the x-axis. One can use a standard perturbation expansion (e.g. Melrose 1986, Ch. 2) in terms of the field amplitudes, by writing the momentum of beam particles as

$$\boldsymbol{p} = \pm\gamma_{\rm b}m_{\rm b}\,V_{\rm b}\,\hat{\boldsymbol{z}} + \boldsymbol{p}_{(1)} + \boldsymbol{p}_{(2)} + \ldots \tag{37}$$

and solving the equation of motion order-by-order. Here $|\boldsymbol{p}_{(n)}| \propto |\tilde{A}|^n$ is the nth order momentum perturbation. A similar expansion can be written down for the velocity: $\boldsymbol{V} = \pm V_{\rm b}\,\hat{\boldsymbol{z}} + \boldsymbol{V}_{(1)} + \boldsymbol{V}_{(2)} + \cdots$, where one must use $\boldsymbol{V} = c\boldsymbol{p}/\sqrt{p^2 + m_{\rm b}^2c^2}$ to relate the terms in the momentum and velocity expansions.

The first-order terms in this expansion can be found written out explicitly in Melrose (1986), p. 18. In our application of the theory we will exploit the fact that there are (by assumption) two small parameters: $1/\gamma_{\rm b} \ll 1$ and $|\omega/kc| \ll 1$. Using this, one finds from the general perturbation expansion that the first-order velocity perturbations in the beam satisfy

$$\left|\frac{\tilde{V}_{(1)\,z}(k\,,\,\omega)}{\tilde{V}_{(1)\,x}(k\,,\,\omega)}\right| = \frac{1}{\gamma_{\rm b}^2}\,\left|\frac{\omega}{kV_{\rm b}}\right| \approx \frac{1}{\gamma_{\rm b}^2}\,\left|\frac{\omega}{kc}\right| \ll 1. \tag{38}$$

Here $\tilde{\boldsymbol{V}}_{(1)}(k\,,\,\omega)$ is the Fourier component of the linear velocity perturbation, defined in a manner analogous to Eq. (35). This implies that one can neglect the wave-induced motion along the beam direction (along the z-axis) to first order. It can be shown that a similar conclusion holds for the higher-order velocity perturbations $\tilde{\boldsymbol{V}}_{(2)}(k\,,\,\omega)\,,\ \tilde{\boldsymbol{V}}_{(3)}(k\,,\,\omega)\ldots$ This allows one to approximate the equation of motion (28) by

$$\left(\frac{\partial}{\partial t} + V_\pm\,\frac{\partial}{\partial x}\right) V_\pm(x\,,\,t) = \frac{q_\mathrm{b}\mathcal{E}_\pm(x\,,\,t)}{\gamma_\mathrm{b} m_\mathrm{b}}\cdot \tag{39}$$

Here we have written $V_\pm(x\,,\,t)$ for the x-component $V_x(x\,,\,t)$ of the velocity for the forward and backward beam. Note that this velocity component vanishes for the unperturbed beam, so that $V_\pm = V_{\pm(1)} + V_{\pm(2)} + \ldots$ in a perturbation expansion. We also define

$$\mathcal{E}_\pm(x\,,\,t) = E_\parallel \mp \frac{V_\mathrm{b}}{c} B \approx E_\parallel \mp B. \tag{40}$$

The last approximation follows from our assumption $\gamma_\mathrm{b} \gg 1$.

The approximate equation of motion (39) neglects the relatively small nonlinear contributions to the Lorentz force due to variations in V_z, and also the equally small nonlinear variations in γ, keeping only the dominant nonlinearity due to ponderomotive effects, which is associated with the advective term, $V_\pm\,(\partial V_\pm/\partial x)$, in the equation of motion (39).

In the same limit, the current density carried by the beams is almost entirely due to the *advection current* that is associated with the charge density perturbations in the beams:

$$\boldsymbol{J}_\mathrm{b} \approx q_\mathrm{b}\,\left(n_+ - n_-\right) V_\mathrm{b}\,\hat{\boldsymbol{e}}_z. \tag{41}$$

The *conduction current*, which is induced by the perturbations in the z-component of the beam velocity, is a factor $\sim|\omega/\gamma_\mathrm{b} kc|^2 \ll 1$ smaller and will be neglected in what follows.

3.2. Reduced set of Maxwell's equations

In the low-frequency limit $|\omega| \ll kc$ one can employ a set of reduced Maxwell equations to describe the plasma response: Ampère's Law neglecting the displacement current, $\boldsymbol{\nabla}\times\boldsymbol{B} = (4\pi/c)\,\boldsymbol{J}$, and Poisson's equation $\boldsymbol{\nabla}\cdot\boldsymbol{E} = 4\pi\rho$ for the longitudinal electric field. Here ρ and $\boldsymbol{J}$ are the charge and current densities. For the moment we will neglect the effect of the background plasma, except as an infinitely massive neutralizing agent that compensates the charge of the beam particles in the unperturbed state, carrying a charge density $\rho_\mathrm{bg} = -q_\mathrm{b}\overline{n}_\mathrm{b}$ in the laboratory frame. In this case Maxwell's equations reduce to

$$\begin{aligned}\frac{\partial E_\parallel}{\partial x} &= 4\pi q_\mathrm{b}\,\left(n_+ + n_- - \overline{n}_\mathrm{b}\right)\\ \frac{\partial B}{\partial x} &= 4\pi q_\mathrm{b}\,\frac{V_\mathrm{b}}{c}\,\left(n_+ - n_-\right) \simeq 4\pi q_\mathrm{b}\,(n_+ - n_-)\,.\end{aligned} \tag{42}$$

Using the definition (40) for $\mathcal{E}_\pm$ one finds that the reduced set of Maxwell's equations is equivalent to

$$\frac{\partial \mathcal{E}_\pm}{\partial x} = 8\pi q_\mathrm{b}\,\left(n_\mp - \tfrac{1}{2}\overline{n}_\mathrm{b}\right). \tag{43}$$

The density of the two beams satisfies the continuity equation:

$$\frac{\partial n_\pm}{\partial t} + \frac{\partial}{\partial x}\,(n_\pm V_\pm) = 0. \tag{44}$$

Together with relation (43) this implies:

$$\frac{\partial^2 \mathcal{E}_\pm}{\partial x \partial t} = -8\pi q_\mathrm{b}\,\frac{\partial}{\partial x}\,(n_\mp V_\mp)\,. \tag{45}$$

This last relation can be integrated to

$$\frac{\partial \mathcal{E}_\pm}{\partial t} = C_\pm(t) - 8\pi q_\mathrm{b} n_\mp V_\mp. \tag{46}$$

Here the $C_\pm(t)$ are arbitrary functions of time, but do not depend on the position x. For waves periodic in x it is easily checked by averaging over one wavelength that these two integration constants must vanish: $C_+ = C_- = 0$. In that case one can combine Eqs. (43) and (46) to show that $\mathcal{E}_+$ and $\mathcal{E}_-$ satisfy:

$$\mathcal{D}_-\mathcal{E}_+ = -4\pi q_\mathrm{b}\overline{n}_\mathrm{b}\,V_-\ \ ,\ \ \mathcal{D}_+\mathcal{E}_- = -4\pi q_\mathrm{b}\overline{n}_\mathrm{b}\,V_+. \tag{47}$$

Here we use the following notation for the convective derivatives associated with the two beams:

$$\mathcal{D}_\pm \equiv \frac{\partial}{\partial t} + V_\pm\,\frac{\partial}{\partial x}\cdot \tag{48}$$

In this notation the equations of motion (39) read:

$$\mathcal{D}_+ V_+ = \frac{q_\mathrm{b}\mathcal{E}_+}{\gamma_\mathrm{b} m_\mathrm{b}}\ \ ,\ \ \mathcal{D}_- V_- = \frac{q_\mathrm{b}\mathcal{E}_-}{\gamma_\mathrm{b} m_\mathrm{b}}\cdot \tag{49}$$

The coupled set of nonlinear Eqs. (47) and (49) describes oscillations in the beam plasma. Note that *all* the nonlinear effects are in the lefthand sides of these four coupled equations: the righthand sides are all linear! The nonlinearities are associated with the $V_\pm(\partial V_\pm/\partial x)$ terms in the convective derivatives $\mathcal{D}_\pm$. Also, these equations exhibit a remarkable symmetry that we will employ below.

By operating with $\mathcal{D}_-$ on the first equation of (49) and with $\mathcal{D}_+$ on the second equation one can reduce the system further: one finds two coupled equations for $V_\pm$:

$$\mathcal{D}_-\mathcal{D}_+ V_+ = -\hat{\omega}_\mathrm{pb}^2\,V_-\ \ ,\ \ \mathcal{D}_+\mathcal{D}_- V_- = -\hat{\omega}_\mathrm{pb}^2\,V_+. \tag{50}$$

Here the *constant* beam plasma frequency is defined as

$$\hat{\omega}_\mathrm{pb}^2 = \frac{4\pi q_\mathrm{b}^2\overline{n}_\mathrm{b}}{\gamma_\mathrm{b} m_\mathrm{b}}\cdot \tag{51}$$

3.3. Linear response of the beam plasma

If one neglects nonlinear effects one can put $\mathcal{D}_+ = \mathcal{D}_- = \partial/\partial t$. The set of two Eqs. (50) is then equivalent with the single equation

$$\frac{\partial^4 V_\pm}{\partial t^4} = \hat{\omega}_\mathrm{pb}^4\,V_\pm, \tag{52}$$

Assuming $V_\pm \propto \exp(\mathrm{i}\omega t)$ one finds that $\omega^4 = \hat{\omega}_\mathrm{pb}^4$, and the solutions are

$$\omega = \pm\hat{\omega}_\mathrm{pb}\ \ ,\ \ \omega = \pm i\hat{\omega}_\mathrm{pb}. \tag{53}$$

The first two solutions are symmetric in the sense that $V_+ = V_-$, as is easily seen by substituting the solution back into the original (linearized) set of equations. In the linear case this implies $\mathcal{E}_+ = \mathcal{E}_-$, so that one must have $E_\parallel \neq 0$ and $B = 0$. These are stable electrostatic (longitudinal) plasma waves in the beam

plasma. The second set of solutions for ω correspond to an exponentially growing and an exponentially decaying mode. Both these solutions are anti-symmetric in the sense that $V_+ = -V_-$. The Weibel instability in the short-wavelength limit corresponds to the growing mode. In this case $\mathcal{E}_+ = -\mathcal{E}_-$, so that one must have $E_\parallel = 0$ and $B \neq 0$, and the waves are transverse. In this limit, where we have assumed that terms of order $|\omega/kc|$ and $1/\gamma_\mathrm{b}$ can be neglected with respect to unity, these two transverse modes are purely magnetic.

3.4. The nonlinear response for single modes: the effect of wave breaking

As argued above, the dominant nonlinearity for $|\omega| \ll kc$ and $\gamma_\mathrm{b} \gg 1$ is associated with the $V_\pm\,(\partial V_\pm/\partial x)$ terms in the convective derivates $\mathcal{D}_\pm$. These terms describe the distortion of the waves from the initial sinusoidal shape by the process of *wave breaking*. One usually defines the displacement of beam particles in the x-direction by

$$\xi_\pm(r_\pm\,,\ t) = x_\pm(t) - r_\pm \quad \text{with} \quad r_\pm \equiv x_\pm(t=0). \tag{54}$$

The $r_\pm$ are Lagrangian labels that are carried along by the particles. The convective derivative and the velocity in the x-direction can be reinterpreted in terms of these labels as (cf. Roberts 1967, Ch. 1.7)

$$\mathcal{D}_\pm = \left(\frac{\partial}{\partial t}\right)_{r_\pm} \quad , \quad V_\pm = \mathcal{D}_\pm \xi_\pm = \left(\frac{\partial \xi_\pm}{\partial t}\right)_{r_\pm} . \tag{55}$$

Using these definitions it follows that the formal solution of the two equations (47) for $\mathcal{E}_\pm$ reads:

$$\begin{aligned} \mathcal{E}_+(r_- + \xi_-\,,\ t) \ &= \ -4\pi q_\mathrm{b} \overline{n}_\mathrm{b}\, \xi_-(r_-\,,\ t), \\ \mathcal{E}_-(r_+ + \xi_+\,,\ t) \ &= \ -4\pi q_\mathrm{b} \overline{n}_\mathrm{b}\, \xi_+(r_+\,,\ t). \end{aligned} \tag{56}$$

This shows that (in this limit) the $\mathcal{E}_+$-field is determined by the motion of the particles in the $-$-beam, and vice versa. This result is important for the rest of the discussion.

Consider now the motion of particles in one of the two beams, say the forward (+) beam. The equation of motion can be written as

$$\left(\frac{\partial^2 \xi_+}{\partial t^2}\right)_{r_+} = \frac{q_\mathrm{b}}{\gamma_\mathrm{b} m_\mathrm{b}}\, \mathcal{E}_+(r_+ + \xi_+\,,\ t). \tag{57}$$

In the linear approximation one puts $r_+ + \xi_+ \approx r_+ \approx r_-$, neglecting the difference between the orbits followed by the particles in the forward and backward beam. Consider now the case of the initial condition $r_+ = r_- \equiv r$. In the linear stage of the Weibel instability one can put

$$\xi_+(r\,,\ t) = -\xi_-(r\,,t) = a(t)\ \sin(kr), \tag{58}$$

which decribes a plane wave in the Lagrangian coordinate r with wavelength $2\pi/k$. The amplitude $a(t)$ grows initially as $a(t) \propto \exp(\hat{\omega}_\mathrm{pb} t)$. As the beam particles move in x, the wave is distorted from its initial sinusoidal shape. From (56) and (58) one has:

$$\begin{aligned} \mathcal{E}_+(r + \xi_+\,,\ t) \ &\approx \ \mathcal{E}_+(r + \xi_- + 2\xi_+\,,\ t) \\ &= \ -4\pi q_\mathrm{b} \overline{n}_\mathrm{b}\, \xi_-(r + 2\xi_+\,,\ t) \\ &\approx \ 4\pi q_\mathrm{b} \overline{n}_\mathrm{b}\, a(t) \sin\left[kr + 2ka(t)\ \sin(kr)\ \right]. \end{aligned} \tag{59}$$

With the help of an expansion in terms of the Bessel functions of integer order[2],

$$\sin(kr + 2ka\ \sin(kr)) = \sum_{m=-\infty}^{\infty} J_m(2ka)\ \sin([m+1]kr), \tag{60}$$

one sees that [1] higher spatial harmonics are generated by the nonlinearity through the $m \neq 0$ terms and [2] that there is a phase shift due to wave breaking, which ultimately slows the instability.

Some insight into the nonlinear development can be gained by considering the initially dominant $m = 0$ term. The motion of the beam particles is approximately described by:

$$\frac{\partial^2 a}{\partial t^2} \approx \hat{\omega}_\mathrm{pb}^2 a(t)\, J_0(2ka(t)), \tag{61}$$

neglecting the higher spatial harmonics (i.e. the terms with $m \neq 0$). Using the property

$$x\, J_0(x) = \frac{\mathrm{d}}{\mathrm{d}x}\,(x\, J_1(x)) \tag{62}$$

of the zero-order Bessel function $J_0(x)$, it is easily checked that Eq. (61) corresponds to motion in a potential, with an energy integral that can be expressed as

$$\frac{1}{2}\left(\frac{\mathrm{d}\tilde{a}}{\mathrm{d}\tilde{t}}\right)^2 + V(\tilde{a}) = \text{const.}, \tag{63}$$

where $\tilde{a} = 2ka$ and $\tilde{t} = \hat{\omega}_\mathrm{pb} t$, and the potential is

$$V(\tilde{a}) = -\tilde{a}\, J_1(\tilde{a}). \tag{64}$$

The form of the potential (see Fig. 2) is such that, after initial almost exponential growth of $a(t)$, a *stable* nonlinear oscillation results whenever the amplitude of the initial perturbation is small. If the instability starts with $|\tilde{a}| \ll 1$ and $|\mathrm{d}\tilde{a}/\mathrm{d}\tilde{t}| \ll 1$, the integration constant in (63) will be close to zero as $V(0) = 0$. In that case the two turning points of the motion of $\tilde{a}$ will be located close to the first zero's of $J_1(\tilde{a})$, which are at

$$|\tilde{a}_\mathrm{max}| = 2k\,|a_\mathrm{max}| \approx 3.83. \tag{65}$$

This simplified analysis predicts that the distortion of the wave profile, together with the relative shift $\Delta\xi = \xi_+ - \xi_- \approx 2\xi_+$ between the orbits of the particles in the two beams, stabilizes the instability, and leads to oscillations with an amplitude

$$|a| \approx \frac{3.83}{2k} \approx 0.3\ \lambda, \tag{66}$$

where $\lambda = 2\pi/k$ is the wavelength of the original perturbation.

This result shows that wave breaking will limit the amplitude of the displacement $\xi_\pm$ of the beam particles, see Eq. (58). Because this displacement is directly related to the electromagnetic fields through Eq. (56), this also yields a limit on the electromagnetic field strength. However, to get an accurate estimate of the resulting magnetic field strength we have to take the influence of the background plasma into account, which we will do in the next section.

[2] This result follows from the better-known expansion $\mathrm{e}^{\mathrm{i}b\,\sin\theta} = \sum_m J_m(b)\,\exp(\mathrm{i}m\theta)$, together with $\sin z = (\mathrm{e}^{\mathrm{i}z} - \mathrm{e}^{-\mathrm{i}z})/2\mathrm{i}$ and $J_m(-b) = (-1)^m\, J_m(b) = J_{-m}(b)$.

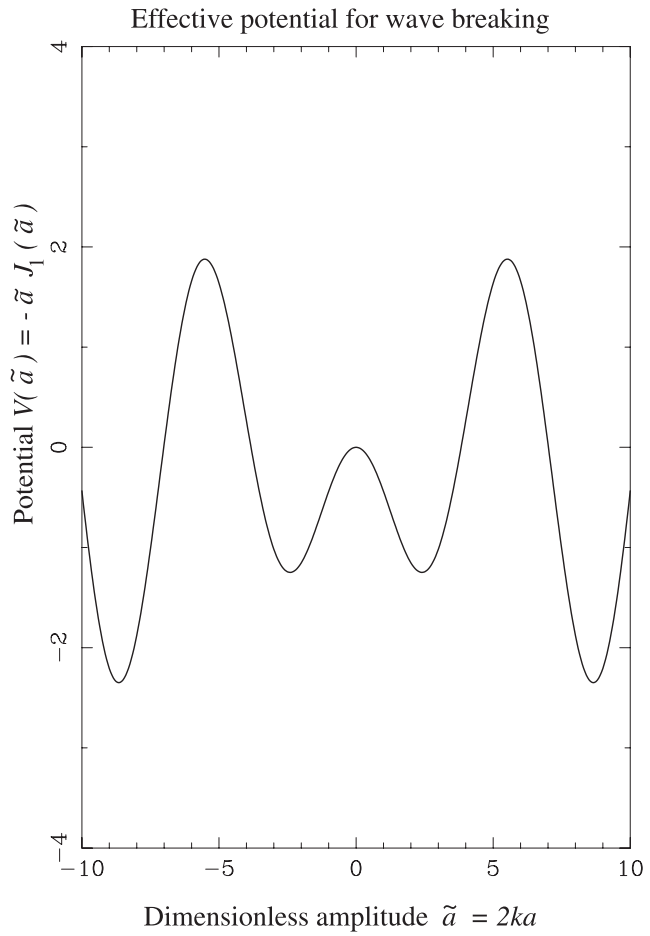

Fig. 2. The potential $V(\tilde{a})$ as function of the dimensionless amplitude $\tilde{a} = 2ka$.

3.5. Influence of the background plasma

So far we have neglected the response of the background plasma, treating it in effect as an infinitely massive neutralizing background. We will now relax this assumption. The main effect of the background is to introduce screening currents and charges that slow the growth of the Weibel instability. We will describe the background as an isotropic plasma. Since the Weibel instability is mainly magnetic, we will only need the transverse response of the plasma. The Fourier-transformed reduced Maxwell equations that include the background response replace the equation for the Fourier-amplitude of the magnetic field, $\mathrm{i}k\,\tilde{B} \simeq 4\pi q_\mathrm{b}\ (\tilde{n}_+ - \tilde{n}_-)$, by

$$\mathrm{i}k\epsilon_\perp(k\ ,\ \omega)\tilde{B} = 4\pi q_\mathrm{b}\ (\tilde{n}_+ - \tilde{n}_-)\,. \tag{67}$$

Here $\epsilon_\perp(k\ ,\ \omega)$ is the transverse response (dielelectric) function of the background plasma. We have again assumed a relativistic beam with $V_\mathrm{b} \simeq c$. In terms of the components α_{ij} of the polarization tensor defined in AW1 (AW1, Eqs. (33) and (34)) one has:

$$\epsilon_\perp(k\ ,\ \omega) = 1 + \frac{\alpha_{33}^{\mathrm{bg}}(k\ ,\ \omega)}{k^2c^2}\cdot \tag{68}$$

It gives the effect of screening currents carried by the background plasma. In the linear approximation, where $\mathcal{E}_+ \approx -\mathcal{E}_- = -B$, Eq. (67) together with the equation of motion and the continuity equation of the beam particles imply that the electromagnetic fields in the Fourier domain that are associated with the unstable Weibel mode now satisfy:

$$\tilde{\mathcal{E}}_\pm(k\ ,\ \omega) \approx -\frac{4\pi q_\mathrm{b}\overline{n}_\mathrm{b}}{\epsilon_\perp(k\ ,\ \omega)}\ \tilde{\xi}_\mp(k\ ,\ \omega)\cdot \tag{69}$$

As shown in AW1, the effect of screening currents can be described in a good approximation by putting

$$\epsilon_\perp(k\ ,\ \omega) \approx \frac{\kappa^2 + \kappa_\mathrm{s}^2}{\kappa^2}, \tag{70}$$

with $\kappa = kc/\tilde{\omega}_\mathrm{bg}$ with $\tilde{\omega}_\mathrm{bg}$ the plasma frequency of the background plasma, and where κ_s is the dimensionless screening wave number. The equation for the *linear* Weibel mode with a given wavelength $\lambda = 2\pi/k$ is then equivalent with

$$\frac{\partial^2\tilde{\xi}_\pm(k\ ,\ t)}{\partial t^2} = \frac{\hat{\omega}_\mathrm{pb}^2}{\epsilon_\perp(k)}\ \tilde{\xi}_\pm(k\ ,\ t). \tag{71}$$

Again this leads to an exponentially growing amplitude, $\tilde{\xi}_\pm(t) \propto \exp(\tilde{\sigma}_\mathrm{W}t)$, where

$$\tilde{\sigma}_\mathrm{W}(k) = \frac{\hat{\omega}_\mathrm{pb}}{\sqrt{\epsilon_\perp(k)}} = \frac{\kappa}{\sqrt{\kappa^2 + \kappa_\mathrm{s}^2}}\ \hat{\omega}_\mathrm{pb}. \tag{72}$$

The factor $1/\sqrt{\epsilon_\perp(k)}$ shows that the background response lowers the growth rate of the linear instability. Expression (72) is exactly the growth rate that follows from Eq. (7) in the case of cold beams ($\mathcal{M} \to \infty$) as considered here. For $\kappa \gg \kappa_\mathrm{s}$ the effect of the background plasma is very small.

The presence of screening currents does not influence the stabilization argument of the previous Section, which is based entirely on the response of the beam particles. The analysis presented there (e.g. Eq. (65)) predicts that the Weibel instability saturates at a level where

$$k\ \left|\tilde{\xi}_\pm\right| \simeq 1.9. \tag{73}$$

From (69) one has

$$\left|\tilde{\mathcal{E}}_\pm\right| \approx \left|\tilde{B}\right| \approx \frac{4\pi q_\mathrm{b}\overline{n}_\mathrm{b}}{\epsilon_\perp(k)}\ \left|\tilde{\xi}_\pm\right| \approx \frac{8\pi q_\mathrm{b}\overline{n}_\mathrm{b}}{k\ \epsilon_\perp(k)}. \tag{74}$$

It is easily checked that this estimate is equivalent to the standard trapping argument.

4. Kinetic theory: stabilization due to quiver motion

We now consider the stabilization of the Weibel instability from the point-of-view of kinetic theory. We assume a *broad-band spectrum* of unstable modes with a bandwidth $\Delta k \sim k$, in contrast to the calculation of the previous Section which assumed a single (dominant) mode.

Such a broad-band spectrum leads to *phase-mixing* of the particle motion (the so-called quiver motion) in the collection of waves. This ultimately results in a broadening of the momentum distribution function $f_\mathrm{b}(\boldsymbol{p})$ of the beam particles in phase space. Traditionally this process is described as "fake diffusion" (e.g. Davidson 1972), where the term "fake" refers to the fact that this process, unlike true diffusion, is in principle *reversible*! In more modern incarnations of the theory of wave-particle interactions one uses *oscillation center theory* to define the average distribution function in the presence of waves, see for instance

Cary & Kaufman (1981). Since the linear Weibel instability has $\mathrm{Re}(\omega) = 0$, there are no resonant nonlinear effects, such as resonant wave-wave coupling as already discussed above, or such typical *kinetic* nonlinear resonant processes, such as nonlinear Landau damping. These processes usually dominate the nonlinear dynamics of plasma waves with $|\mathrm{Re}(\omega)| \gg |\mathrm{Im}(\omega)|$.

This broadening of the momentum distribution effectively heats the plasma and it is well known that heating of the plasma will stabilize the Weibel instability. In this section we will first estimate the broadening of the velocity distribution in terms of the amplitude of the magnetic field generated by the instability. Using this estimate we will calculate the effect on the response of the beam particles and derive the magnetic field strength at the point where the broadening slows down the instability appreciably.

4.1. Broadening of the momentum distribution

Once again we consider the case of two counterstreaming and ultra-relativistic beams that propagate along the z-axis. The dispersion relation for the Weibel instability as derived in AW1 reads, in the limit $|\omega^2| \ll k^2c^2$:

$$c^2k^2 + \alpha_{33}^{\rm bg}(\omega\,,\,k) + \alpha_{33}^{\rm b}(\omega\,,\,k) = 0, \tag{75}$$

where the polarization tensor component α_{33} has a contribution $\alpha_{33}^{\rm bg}(\omega,k)$ due to the background plasma, and $\alpha_{33}^{\rm b}(\omega,k)$ due to the beams. The last contribution is (AW1, Appendix, Eq. (C7)):

$$\begin{aligned}\alpha_{33}^{\rm b}(\omega\,,\,k) \;=\; & \frac{4\pi q_{\rm b}^2\overline{n}_{\rm b}}{m_{\rm b}} \int \frac{{\rm d}^3\boldsymbol{p}}{\gamma(\boldsymbol{p})}\, f_{0\rm b}(\boldsymbol{p}) \left(1 - \frac{v_z^2}{c^2}\right) \\ & -4\pi q_{\rm b}^2\overline{n}_{\rm b} \int {\rm d}^3\boldsymbol{p} \left\{\frac{v_z^2}{\omega - kv_x} \left(k\,\frac{\partial f_{0\rm b}(\boldsymbol{p})}{\partial p_x}\right)\right\}. \end{aligned} \tag{76}$$

Here $f_{0\rm b}(\boldsymbol{p})$ is the average phase-space density of the beam particles, normalized to

$$\int {\rm d}^3\boldsymbol{p}\, f_{0\rm b}(\boldsymbol{p}) = 1, \tag{77}$$

and $\gamma(\boldsymbol{p}) = \sqrt{1 + |\boldsymbol{p}|^2/m_{\rm b}^2c^2}$.

The effect of the quiver motion is a broadening of the mean distribution function. We will denote the spatially averaged distribution function of the beam particles by $f_{0\rm b}$, to be distinguished from the exact distribution $f_{\rm b}$, which includes a fluctuating part. In the limit $|\omega| \ll kc$ and for $\boldsymbol{k} = k\hat{\boldsymbol{x}}$ and $\boldsymbol{B} = B\,\hat{\boldsymbol{y}}$ the Vlasov equation for the exact distribution $f_{\rm b}(\boldsymbol{x}\,,\,t\,,\,\boldsymbol{p})$ can be approximated by

$$\frac{\partial f_{\rm b}}{\partial t} + v_x\,\frac{\partial f_{\rm b}}{\partial x} - \left(\frac{q_{\rm b}\,v_z B}{c}\right)\frac{\partial f_{\rm b}}{\partial p_x} = 0. \tag{78}$$

Here $f_{\rm b}(x\,,\,t\,,\,p_x\,,p_y\,,\,P_z)$ is taken to be a function of the x-coordinate and time, of the momentum components p_x and p_y perpendicular to the beam direction (which equal the canonical momentum components P_x and P_y because $A_x = A_y = 0$) and the (conserved) canonical momentum $P_z = p_z + q_{\rm b}A/c$. Using standard techniques of weak plasma turbulence (e.g. Davidson 1972, Ch. 8), one can show that the mean distribution function $f_{0\rm b}$ satisfies a diffusion equation of the form

$$\frac{\partial f_{0\rm b}}{\partial t} = \frac{\partial}{\partial p_x}\left\{\left(\frac{q_{\rm b}v_z}{c}\right)^2 \int \frac{{\rm d}k\,{\rm d}\omega}{(2\pi)^2}\,\frac{\tilde{\sigma}\,\left\langle|\tilde{B}(k\,,\,\omega)|^2\right\rangle}{(\omega_{\rm r} - kv_x)^2 + \tilde{\sigma}^2}\,\frac{\partial f_{0\rm b}}{\partial p_x}\right\}. \tag{79}$$

This equation gives the effect of the quiver motion on the mean distribution function. Here the wave frequency is written in terms of its real and imaginary part as $\omega(k) = \omega_{\rm r} + {\rm i}\tilde{\sigma}$. For a broad-band spectrum of normal modes the ensemble average satisfies

$$\left\langle|\tilde{B}(k\,,\,\omega)|^2\right\rangle = \tilde{B}^2(k)\,2\pi\delta(\omega - \omega(k)), \tag{80}$$

with $\omega(k)$ the wave frequency as determined by the solution of the dispersion relation (75).

We now make the assumption of beams that are initially cold in the direction perpendicular to the beam direction so that $|kv_x| \ll |\omega|$. In the linear stage of the Weibel instability the amplitude of the magnetic perturbations grows as

$$\frac{\partial\tilde{B}^2(k)}{\partial t} = 2\tilde{\sigma}(k)\,\tilde{B}^2(k), \tag{81}$$

and $\omega_{\rm r} = \mathrm{Re}(\omega) = 0$. In this limit, Eq. (79) can be approximated by

$$\frac{\partial f_{0\rm b}}{\partial t} = \int \frac{{\rm d}k}{2\pi}\,\frac{\partial\tilde{B}^2(k)}{\partial t}\left(\frac{\partial}{\partial p_x}\left\{\frac{q_{\rm b}^2v_z^2}{2\tilde{\sigma}^2c^2}\,\frac{\partial f_{0\rm b}}{\partial p_x}\right\}\right). \tag{82}$$

The linear growth rate $\tilde{\sigma}(k)$ is almost independent of wave number for $1 < kc/\tilde{\omega}_{\rm bg} < \kappa_{\max}$. In addition we have $f_{0\rm b} \propto \delta(P_z + \gamma_{\rm b}m_{\rm b}V_{\rm b}) + \delta(P_z - \gamma_{\rm b}m_{\rm b}V_{\rm b})$ (see Eq. (34)) and $p_z \approx P_z$, so we can put $v_z = \pm V_{\rm b}$. We define the typical magnetic field strength B by the relation

$$B^2 = \int \frac{{\rm d}k}{2\pi}\,\tilde{B}^2(k). \tag{83}$$

Together, Eqs. (81)–(83) and the properties of $\tilde{\sigma}(k)$ imply that $f_{0\rm b}$ satisfies a diffusion equation of the form:

$$\frac{\partial f_{0\rm b}}{\partial(B^2)} = \frac{\partial f_{0\rm b}/\partial t}{\partial(B^2)/\partial t} = \frac{\partial}{\partial p_x}\left\{\frac{q_{\rm b}^2V_{\rm b}^2}{2\tilde{\sigma}^2c^2}\,\frac{\partial f_{0\rm b}}{\partial p_x}\right\}. \tag{84}$$

If the beams are ultra-relativistic and cold at $t = 0$, the momentum distribution is given by:

$$\begin{aligned} f_{0\rm b}(t=0) \;=\; & \delta(p_x)\,\delta(p_y) \\ & \times\tfrac{1}{2}\left[\delta(P_z + \gamma_{\rm b}m_{\rm b}V_{\rm b}) + \delta(P_z - \gamma_{\rm b}m_{\rm b}V_{\rm b})\right]. \end{aligned} \tag{85}$$

Using $\gamma_{\rm b} \gg 1$ the solution to Eq. (84) can then be written as a quasi-Maxwellian distribution in $v_x = p_x/\gamma_{\rm b}m_{\rm b}$:

$$\begin{aligned} f_{0\rm b}(t) \;=\; & \frac{1}{\sqrt{2\pi}\,\gamma_{\rm b}m_{\rm b}v_{\rm q}}\,{\rm e}^{-(v_x^2/2v_{\rm q}^2)}\;\delta(p_y) \\ & \times\tfrac{1}{2}\left[\delta(P_z + \gamma_{\rm b}m_{\rm b}V_{\rm b}) + \delta(P_z - \gamma_{\rm b}m_{\rm b}V_{\rm b})\right]. \end{aligned} \tag{86}$$

Here the quiver velocity $v_{\rm q}$ is defined by:

$$v_{\rm q}^2 \approx \frac{q_{\rm b}^2V_{\rm b}^2B^2}{2\gamma_{\rm b}^2m_{\rm b}^2\tilde{\sigma}^2c^2}. \tag{87}$$

This explicitly shows how the mean distribution in v_x (with associated momentum $p_x \approx \gamma_{\rm b}m_{\rm b}v_x$) broadens due to phase mixing of the quiver motion as the rms magnetic field grows. The above procedure generalizes a similar result derived by Kadomtsev (1965), p. 25, for electrostatic waves.

If we relax the assumption that the wave vector $\boldsymbol{k}$ is in the x-direction, and allow for $k_y \neq 0$, $B_x \neq 0$ while keeping $k_z = 0$, a

similar broadening occurs in the distribution of the y-component of momentum. If the situation is cylindrically symmetric around the beam direction, with

$$\tilde{B}_x^2(k) = \tilde{B}_y^2(k) \equiv \tilde{B}^2(k), \tag{88}$$

expression (86) is replaced by

$$f_{0\mathrm{b}}(t) \;=\; \frac{1}{2\pi\,(\gamma_\mathrm{b} m_\mathrm{b}\, v_\mathrm{q})^2}\,\mathrm{e}^{-(v_x^2+v_y^2)/2v_\mathrm{q}^2} \times\tfrac{1}{2}\left[\delta(P_z+\gamma_\mathrm{b} m_\mathrm{b} V_\mathrm{b})+\delta(P_z-\gamma_\mathrm{b} m_\mathrm{b} V_\mathrm{b})\right]. \tag{89}$$

In conclusion: the effect of the phase mixing of the quiver motion is to heat the beam plasma, in particular by creating a quasi-Maxwellian distribution of the components of the particle momentum in the $x-y$-plane, the plane perpendicular to the beam direction.

4.2. Effect on the beam response

The change in the beam momentum distribution also changes the contribution of the beam to the polarization tensor component $\alpha_{33}(\omega\,,\,k)$ that figures in the dispersion relation for the Weibel instability. Using distribution function (89) in definition (76) gives the beam contribution to α_{33} in the limit $v_\mathrm{q} \ll c$ so that $p_x \approx \gamma_\mathrm{b} m_\mathrm{b} v_x$:

$$\alpha_{33}^\mathrm{b} = \hat{\omega}_\mathrm{pb}^2\left(\frac{1}{\gamma_\mathrm{b}^2}+\frac{4v_\mathrm{q}^2}{c^2}\right)-\hat{\omega}_\mathrm{pb}^2\,\frac{k^2V_\mathrm{b}^2}{\omega^2}\,Z^2\,W(Z). \tag{90}$$

Here $Z \equiv \omega/kv_\mathrm{q}$ and $W(Z)$ is the plasma dispersion function defined by Ichimaru (1973),

$$W(Z) \equiv \frac{1}{\sqrt{2\pi}}\int_{-\infty}^{+\infty}\mathrm{d}x\,\frac{x\exp\left(-x^2/2\right)}{x-Z}, \tag{91}$$

and $\hat{\omega}_\mathrm{pb}^2 = 4\pi q_\mathrm{b}^2\overline{n}_\mathrm{b}/\gamma_\mathrm{b} m_\mathrm{b}$ is the effective plasma frequency associated with the beams. To obtain result (90) we have used

$$1-\frac{v_z^2}{c^2} = \frac{1}{\gamma^2}+\frac{v_x^2}{c^2}+\frac{v_y^2}{c^2}\cdot \tag{92}$$

Initially $v_\mathrm{q} \ll |\omega/k| \ll c$ and $|Z| \gg 1$, and we can use the expansion (valid for $\tilde{\sigma} = \mathrm{Im}(\omega) > 0$):

$$W(Z) \approx -\frac{1}{Z^2}-\frac{3}{Z^4}\cdot \tag{93}$$

For $kV_\mathrm{b} \sim kc \gg |\omega|$, $\gamma_\mathrm{b} \gg 1$ and $v_\mathrm{q} \ll c$ we can neglect the first term in (90), and the dispersion relation (75) can be approximated by:

$$k^2c^2+\alpha_{33}^\mathrm{bg}(\mathrm{i}\tilde{\sigma}\,,\,k)-\hat{\omega}_\mathrm{pb}^2\,\frac{k^2V_\mathrm{b}^2}{\tilde{\sigma}^2}\left(1-\frac{3k^2v_\mathrm{q}^2}{\tilde{\sigma}^2}\right)=0. \tag{94}$$

Here we put $\omega = \mathrm{i}\tilde{\sigma}$. This approximate dispersion relation shows that the instability slows down appreciably if $kv_\mathrm{q} \sim \tilde{\sigma}$, or equivalently when

$$\frac{kv_\mathrm{q}}{\tilde{\sigma}} \approx \frac{kq_\mathrm{b}V_\mathrm{b}B}{\gamma_\mathrm{b} m_\mathrm{b} c\tilde{\sigma}^2} \approx 1. \tag{95}$$

This is essentially the trapping criterion (15), with the quiver amplitude $\xi_\mathrm{q} = v_\mathrm{q}/\tilde{\sigma}$ as the typical amplitude. A similar argument for the stabilization of the Weibel instability has been proposed previously by Gruzinov (2001). A more precise evaluation of the dispersion relation using expression (90) for α_{33}^b needs an evaluation of $W(Z) = W(\omega/kv_\mathrm{q})$ in the complex plane, and is beyond the scope of this paper.

5. Further field growth through current channel coalescence

Once trapping finishes the quasi-exponential growth of the magnetic field, further field amplification is still possible. The numerical simulations of Lee & Lampe (1973), and more recently by Frederiksen et al. (2004) show how the filamentary currents generated by the Weibel instability merge into larger current channels. Physically, this coalescence is the result of the attractive force between parallel currents. Medvedev et al. (2005) have considered a simple model of this coalescence phase, assuming that the process can be approximated by treating the current channels as thin, straight current wires with a magnetic field at a distance r from the wire axis equal to $B(r) = 2I/cr$. Their calculation neglects the screening currents of a background plasma which, at least in the exponential stage of the instability, play an important role in determining the wave number $k_\dagger$ at which the trapping field reaches the maximum value (see Eq. (18)).

In this section we will include the effect of screening currents. In particular, we investigate how the presence of the hot background plasma influences the coalescence process. We will show that the screening currents supported by this background slow the coalescence process considerably once the typical transverse size of the current channels becomes comparable with the skin depth, $c/\tilde{\omega}_\mathrm{bg}$, of the hot background. Even though we (like others before us) will consider the merging of straight and parallel current filaments, the general conclusions should remain qualitatively correct for curved filaments as long as the radius of curvature is considerably larger than both the skin depth of the background plasma and the transverse size of the filaments.

5.1. Maximum current for a cylindrical current channel: the Alfvén current

Following Kato (2005) we define typical currents and the associated magnetic fields for a straight, cylindrical current filament of a given radius r_0. A filament consisting of charged particles with lab frame density $\overline{n}_\mathrm{b}$, charge q_b per particle and with a bulk velocity V_b can carry a maximum current equal to $\mathcal{I}_\mathrm{b} = \pi r_0^2 q_\mathrm{b}\overline{n}_\mathrm{b}V_\mathrm{b}$. If the current channels result from the Weibel instability, the typical size of the channels will be $r_0 \le c/\tilde{\omega}_\mathrm{bg}$. If one neglects screening currents, the typical magnetic field at the outer edge of the filament is

$$B_\mathrm{b} = \frac{2\mathcal{I}_\mathrm{b}}{cr_0} = \frac{2\pi q_\mathrm{b}\overline{n}_\mathrm{b}c}{\tilde{\omega}_\mathrm{bg}}\left(\frac{V_\mathrm{b}}{c}\right)\left(\frac{r_0}{(c/\tilde{\omega}_\mathrm{bg})}\right)\cdot \tag{96}$$

The Alfvén current follows (up to factors of order unity) from the requirement that the gyration radius $r_\mathrm{g} = \gamma_\mathrm{b} m_\mathrm{b} c V_\mathrm{b}/q_\mathrm{b} B$ of the beam particles with an energy $E = \gamma_\mathrm{b} m_\mathrm{b} c^2$ in the self-generated magnetic field B becomes equal to the radius r_0 of the current channel. This gives the critical Alfvén current, $\mathcal{I}_\mathrm{A} = cBr_\mathrm{g}/2 = \gamma_\mathrm{b} m_\mathrm{b} c^2 V_\mathrm{b}/2q_\mathrm{b}$. The associated magnetic field is equal to

$$B_\mathrm{A} = \frac{2\mathcal{I}_\mathrm{A}}{cr_0} = \frac{4\pi q_\mathrm{b}\overline{n}_\mathrm{b}c}{\tilde{\omega}_\mathrm{bg}}\left(\frac{\tilde{\omega}_\mathrm{bg}^2}{\hat{\omega}_\mathrm{pb}^2}\right)\left(\frac{V_\mathrm{b}}{c}\right)\left(\frac{r_0}{(c/\tilde{\omega}_\mathrm{bg})}\right)^{-1}\cdot \tag{97}$$

One has $B_\mathrm{b}(r_0) < B_\mathrm{A}(r_0)$ for $r_0 < \sqrt{2}\,(c/\hat{\omega}_\mathrm{pb})$. Once the current reaches the Alfvén current, the Lorentz force due to the self-generated magnetic field disrupts the current flow.

The trapping condition (15) implies that the magnetic field amplitude for a wave mode with a wave number $k = 2\pi/\lambda$

at the end of the phase of exponential growth is $B^{\rm tr}(k) = \gamma_{\rm b} m_{\rm b} c\tilde{\sigma}^2/q_{\rm b}kV_{\rm b}$. This trapping field serves as an initial condition for the coalescence phase of magnetic field growth (or decay). Using the expression for the growth rate $\tilde{\sigma}(k)$ of the Weibel instability in the ultra-relativistic limit[3], Eq. (7), one has for $k \ll k_{\rm max}$, $h_{\rm b} \approx 1$ (cold beam) and $V_{\rm b} \approx c$:

$$B^{\rm tr}(k) \approx \frac{4\pi q_{\rm b}\gamma_{\rm b} n_{\rm b}}{k}\left(\frac{k^2}{k^2+k_{\rm s}^2}\right). \tag{98}$$

The maximum field amplitude occurs at a wave number close to the screening wave number: $k \sim k_\dagger \sim k_{\rm s} = \tilde{\omega}_{\rm bg}\kappa_{\rm s}/c$. For typical parameters (see below) one has $\kappa_{\rm s} \approx 0.25{-}1$. For the order-of-magnitude estimates we will use the fluid result: $\kappa_{\rm s} = 1$. Note that the field amplitude $B^{\rm tr}$ is *independent* of the mass of the beam particles for $k \gg k_{\rm s}$.

For relativistic beams with $V_{\rm b} \approx c$, and for a wave number $k \geq k_{\rm s} \simeq \tilde{\omega}_{\rm bg}/c$, the magnetic field amplitudes (96) to (98) are related by:

$$B_{\rm b}(r_0) \sim B^{\rm tr}(k = 1/r_0) \;\;,\;\; B_{\rm A}(r_0) \sim \frac{B^{\rm tr}(k=1/r_0)}{\eta(\tilde{\omega}_{\rm bg}r_0/c)^2}. \tag{99}$$

Here we have used definition (2) for η. The current channels created by the Weibel instability typically have $r_0 \sim 1/k_\dagger \leq c/\tilde{\omega}_{\rm bg}$. Relation (99) has immediate consequences for the coalescence of the current filaments created by the Weibel instability that we will explore in Sect. 6.

5.2. Simple model for field growth

The algebraic (rather than exponential) growth of the small-scale field due to merging can be estimated using the toy model for current merging of Medvedev et al. (2005). This model considers the merging of identical and cylindrical current channels. After m pair wise mergers of currents with the same initial scale r_0, current $\mathcal{I}_0$ and magnetic field $B_0 = 2\mathcal{I}_0/cr_0$, the resulting current filament carries a current $\mathcal{I}_m$, has a radius r_m, a cross-section πr_m^2 and a magnetic field $B_m = 2\mathcal{I}_m/cr_m$ at its outer edge. These are given by (Medvedev et al. 2005):

$$\mathcal{I}_m = 2^m\,\mathcal{I}_0 \;\;,\;\; r_m = 2^{m/2}\,r_0 \;\;,\;\; B_m = 2^{m/2}\,B_0. \tag{100}$$

This calculation neglects screening currents, which is a reasonable approximation for $r_m \ll c/\tilde{\omega}_{\rm bg}$, and uses mass conservation and magnetic flux conservation. Combining the last two relations of (100) one has

$$B_m = \left(\frac{r_m}{r_0}\right) B_0. \tag{101}$$

We first consider the merging of electron current filaments following the exponential stage of the electron-driven Weibel instability. At this stage the electrons are already (partially) thermalized, and $\eta \approx 1$, see also the discussion in Sect. 6 below. Using as an initial condition for the merger process the trapping field generated by the Weibel instability, $B_0 = B_{\rm tr}(k = 1/r_0) \approx B_{\rm b}(r_0)$, this yields for $r_m \leq c/\tilde{\omega}_{\rm bg}$:

$$B_m = \frac{2\pi q_{\rm b}\overline{n}_{\rm b} c}{\tilde{\omega}_{\rm bg}}\left(\frac{\tilde{\omega}_{\rm bg} r_m}{c}\right) \approx B_{\rm b}(r_m) \approx B^{\rm tr}(k \sim 1/r_m). \tag{102}$$

[3] Although formally expression (7) for the growth rate $\tilde{\sigma}$ has been derived under the assumption $\tilde{\sigma} \ll kc$, it turns out that it gives a good approximation even if $\tilde{\sigma} \sim kc$.

This simple merging model gives a magnetic field of the merged current filaments of transverse size r_m that is comparable with the trapping field on the same scale, which is the field originally created by the exponential Weibel instability on that scale. When, after multiple mergers, the radius of the resulting filament becomes comparable with the skin depth, $r_m \sim c/\tilde{\omega}_{\rm bg}$, the Alfvén limit $B^{\rm tr}(r = c/\tilde{\omega}_{\rm bg}) \sim B_{\rm A}$ is reached as $\tilde{\omega}_{\rm bg} \sim \hat{\omega}_{\rm pb}$ for the electrons. The electron current cannot grow beyond the (radius-independent) Alfvén limit $\mathcal{I}_{\rm A}^{\rm e} = \gamma_{\rm b} m_{\rm e} c^3/2e$, and the associated magnetic field (see Eq. (97)) will decay as r_m^{-1} if merging continues.

We will argue below that further merging to filaments of a transverse size larger than the skin depth is slowed down considerably by the screening currents generated in the already thermalized hot electron plasma. This means that, for all intents and purposes, the merging almost stops when $r_m \sim c/\tilde{\omega}_{\rm bg}$ when the magnetic field has a magnitude $B_{\rm b} \sim B_{\rm A} \sim B^{\rm tr}$. The decay of the field due to further merging, $B_m \propto r_m^{-1}$ for $B_m > B_{\rm A}$, is present, but proceeds at a much slower rate than the growth of the field in the Weibel instability.

The proton-driven Weibel instability develops much slower, and in a background of already thermalized (hot) electrons, with a the growth rate $\tilde{\sigma} \leq \hat{\omega}_{\rm pb} = \eta\tilde{\omega}_{\rm bg}$ with $\eta \sim m_{\rm e}/m_{\rm p} \ll 1$. This means that the Alfvén field associated with proton currents satisfies $B_{\rm A} \sim B^{\rm tr}/\eta \gg B^{\rm tr}$ at $r \simeq c/\tilde{\omega}_{\rm bg}$. Merging of proton current filaments could therefore in principle lead to continuing magnetic field growth. However, the screening currents act here also, slowing down the merging rate. Therefore, as we will show below, the additional field growth driven by protons or other ions will be limited.

5.3. The effect of screening currents

In shock transition layers one expects a background of hot (already shocked) plasma. This plasma supports screening currents that will partially screen the currents carried by the filamentary beams created by the Weibel instability. This will happen when the transverse size of the current filaments (and their mutual distance) exceeds the skin depth $c/\tilde{\omega}_{\rm bg}$, which is usually determined by the electron component in the hot background. As shown in the Appendix, a simple (quasi-static) model predicts that the magnetic field $B(r)$ and total (beam + screening) current $\mathcal{I}_{\rm tot}$ of a current filament with cylindrical radius r_0 behave for sufficiently thick filaments as (see Eqs. (A.9) and (A.10)):

$$\mathcal{I}_{\rm tot} \simeq \frac{\mathcal{I}_0}{k_{\rm s} r_0} \;\;,\;\; B(r) \simeq B_0\,\frac{e^{-k_{\rm s}(r-r_0)}}{k_{\rm s}\,\sqrt{rr_0}}. \tag{103}$$

Here $k_{\rm s} = \tilde{\omega}_{\rm bg}/c$ is the inverse skin depth and we assume $k_{\rm s} r \gg 1$ and $k_{\rm s} r_0 \gg 1$ with r the distance to the filament axis. The current $\mathcal{I}_0$ is the *unscreened* beam current running through the filament, and $B_0 = 2\mathcal{I}_0/cr_0$. More general expressions for arbitrary values of $k_{\rm s} r$, $k_{\rm s} r_0$ can be found in the Appendix.

The quasi-exponential decay of the magnetic field outside a filament has an important consequence: it slows down the merging of current filaments which is driven by the attractive Lorentz force between filaments with parallel current directions. The attractive force per unit length between two identical filaments of radius $r_0 \gg c/\tilde{\omega}_{\rm bg}$ at a distance $d \gg r_0$ scales roughly as:

$$\frac{{\rm d}F}{{\rm d}\ell} \simeq -\frac{\mathcal{I}_{\rm tot}B(d)}{c} \simeq \left(\frac{{\rm d}F}{{\rm d}\ell}\right)_0 \left(\frac{d}{r_0}\right)^{1/2} \frac{{\rm e}^{-k_{\rm s}(d-r_0)}}{k_{\rm s}^2\,r_0^2}. \tag{104}$$

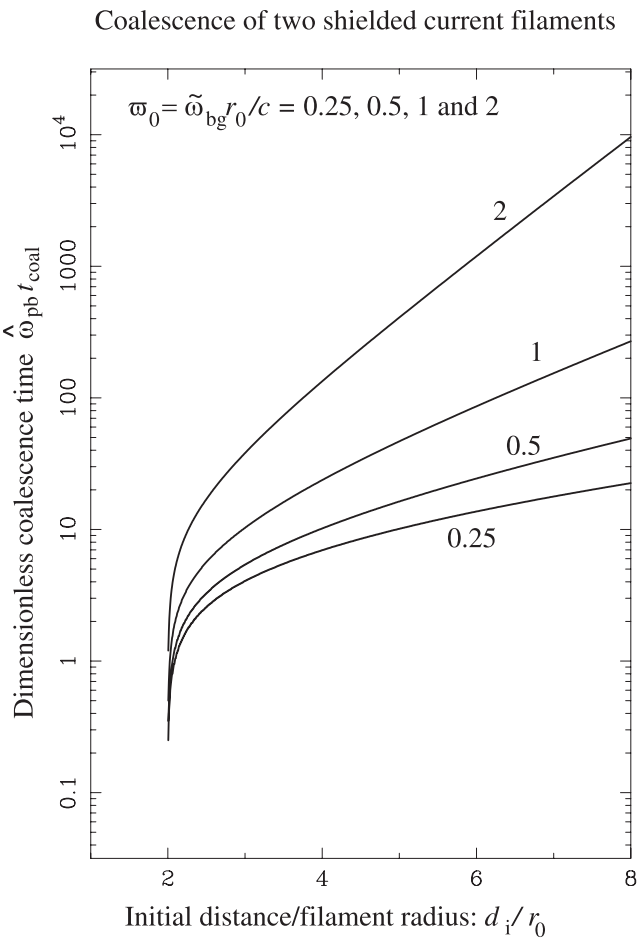

Fig. 3. The coalescence time, plotted as $\hat{\omega}_{\rm pb}\ t_{\rm coal}$, as a function of the distance between the current wires in units of their radius $d_{\rm i}/r_0$. It is assumed that the beam consists of heavy ions with a current equal to $I_{\rm b}$, so that $B_0 \approx B_{\rm b} \approx B_{\rm tr}$, and that $V_{\rm b} \approx c$. Note that for large distances the coalescence time increases exponentially, in agreement with the asymptotic result of Eq. (105).

Here $({\rm d}F/{\rm d}\ell)_0 = -2\,\mathcal{I}_0^2/c^2 d$ is the Biot-Savart attractive force between two thin, unshielded current wires with current $\mathcal{I}_0$, see Eq. (A.11) in the Appendix. As a result, the coalescence time of two identical filaments of radius r_0 also scales quasi-exponentially with the initial distance $d_{\rm i}$ between the filament axes: solving the equation of motion gives in the limit $k_{\rm s} d_{\rm i} \gg k_{\rm s} r_0 \gg 1$ (Appendix, Eq. (A.26) for $B_0 = B_{\rm b}$ and $V_{\rm b} \simeq c$):

$$t_{\rm coal} \simeq \frac{2\pi}{\hat{\omega}_{\rm pb}} \left(k_{\rm s}^2 d_{\rm i} r_0\right)^{1/4} \exp\left[k_{\rm s}\left(\frac{d_{\rm i} - 2r_0}{2}\right)\right]. \qquad (105)$$

The end of the coalescence is taken to be the moment when the filaments touch so that $d = 2r_0$. This behavior is illustrated in Fig. 3, which was obtained through direct numerical integration of the equation of motion (Eq. (A.13) of the Appendix) for $B_0 = B_{\rm b}$, $V_{\rm b} \approx c$.

These calculations imply that the coalescence slows down appreciably as soon as the distance between current filaments exceeds the skin depth of the hot background, $k_{\rm s} d_{\rm i} > 1$. Note that in the simple model of Medvedev et al. (2005) the distance between pair-wise merging current wires increases as $d_m = 2^m d_0$ after the mth merger, if the process starts with an initial collection of wires that are separated by a distance d_0. The ratio of the distance between the wires and their radius scales therefore as $d_m/r_m \propto 2^{m/2}$. This means that, as soon as screening currents become important when $k_{\rm s} r_m \sim 1$, the coalescence rate slows rapidly in the following steps of the merger process, and the coalescence of current filaments effectively "stalls" after a few additional steps.

This simple model assumes that the current filaments remain straight during the merging process. It has been argued by Milosavljević & Nakar (2006) that the filament created by the Weibel instability are unstable to a kink mode, which grows rapidly. These authors use the MHD energy principle to show that a *single* isolated filament with a transverse size of order the plasma skin depth is unstable. It is not clear if this conclusion remains unchanged in the situation considered here, where many filaments interact electromagnetically. The analysis of Milosavljević & Nakar (2006) also does not take account of the effect of the screening currents that one expects around the filaments, which electromagnetically couples the surrounding plasma to the filaments.

6. Implications for ultra-relativistic shocks

We now consider the implications of the results of the previous sections for the generation of magnetic fields near ultra-relativistic shocks. In particular we discuss the shock transition layer, where the kinetic energy of the incoming ions (with mass $m_{\rm i}$) and electrons (and possibly positrons, both with mass $m_{\rm e}$) is thermalized, creating a relativistically hot plasma. Since we are dealing with a collisionless plasma, the behavior of the ions and electrons must be considered separately.

6.1. Thermalization through the Weibel instability

We first consider the effect of the electron-driven Weibel instability. Simulations (e.g. Frederiksen et al. 2004) show that the electron-driven Weibel instability develops rapidly in a shock transition. The ion-driven instability also occurs, but has a maximum growth rate that is a factor $(\hat{\omega}_{\rm pb})_{\rm e}/(\hat{\omega}_{\rm pb})_{\rm p} \approx \sqrt{m_{\rm p}/m_{\rm e}} \sim 43$ slower than the electron-driven instability. Here we assume a hydrogen plasma with the ion mass equal to the proton mass: $m_{\rm i} = m_{\rm p}$. Incidentally: simulations often use (for computational reasons) a much smaller ion-electron mass ratio, of the order $m_{\rm i}/m_{\rm e} \sim 16$ corresponding to $\sqrt{m_{\rm i}/m_{\rm e}} \sim 4$. Therefore, difference in the growth rates of the electron- and ion-driven instabilities is not nearly as pronounced in these simulations as in reality.

If the electrons form their own "subshock", the shock jump conditions should apply to the electron fluid. For ultra-relativistic shocks, where the incoming flow in the shock frame has a Lorentz factor $\gamma_{\rm sh} \gg 1$ and the incoming electron gas is cold in the sense that $k_{\rm b} T_1 \ll m_{\rm e} c^2$, the relation for the relative velocity $v_{\rm rel} = (v_1 - v_2)(1 - v_1 v_2/c^2)$ between the up- and downstream flow is purely kinematic, cf. Blandford & McKee (1976). The corresponding Lorentz-factor is $\gamma_{\rm rel} \simeq \gamma_{\rm sh}/\sqrt{2}$ with $\gamma_{\rm sh} = 1/\sqrt{1 - v_1^2/c^2}$, independent of the mass of the particles that make up the plasma. It is natural to associate $\gamma_{\rm rel}$ with the beam Lorentz factor $\gamma_{\rm b}$ in the rest of the discussion. For $\gamma_{\rm sh} \gg 1$ proper densities on both sides of the shock are related by $n_2/n_1 \simeq 4\,\gamma_{\rm rel}$, and the downstream temperature T_2 follows from $e_2 \simeq 3P_2 = 3 n_2 k_{\rm b} T_2 \simeq \gamma_{\rm rel} n_2 m c^2$, with m the rest mass of the particles involved. For electrons or positrons this implies $k_{\rm b} T_2 \approx \gamma_{\rm rel} m_{\rm e} c^2/3$. Here we have used a subscript 1 (2) to denote the pre-shock (post-shock) state. Below we will take these post-shock values as indicative values for the electron background after thermalization.

Initially, the electron-driven Weibel instability will proceed almost as in the case of no background, the limit $\eta \gg 1$, or equivalently $(\hat{\omega}_{\rm pb})_{\rm e}^2 \gg \tilde{\omega}_{\rm bg}^2$. This implies that the instability grows over a wide range of wavelengths, with a growth rate $\tilde{\sigma} \simeq (\hat{\omega}_{\rm pb})_{\rm e}$. As the beam(s) get further and further behind the shock front, the quiver motion in the self-generated magnetic field will grow in amplitude, and the electron-driven instability starts to stabilize. The typical amplitude of the magnetic field (Eq. (98)) for perturbations with wavelength $\lambda = 2\pi/k$ equals, with $V_{\rm b} \simeq c$

$$B \sim B^{\rm tr} \approx \frac{4\pi e \gamma_{\rm b} n_{\rm e}}{k}. \tag{106}$$

where $n_{\rm e} \approx n_1$ is the proper density of the electron beams and where we have put $h_{\rm e} = 1$ as the electrons are initially cold. The amplitude of the quiver velocity that corresponds with this field amplitude is quite large. From the approximate expression (87) with $\tilde{\sigma} = (\hat{\omega}_{\rm pb})_{\rm e}$ and $V_{\rm b} \simeq c$ one finds

$$\left(\frac{v_{\rm q}}{c}\right)_{\rm e} \sim \frac{(\hat{\omega}_{\rm pb})_{\rm e}}{\sqrt{2}\,kc}, \tag{107}$$

which is of order unity for $k \sim (\hat{\omega}_{\rm pb})_{\rm e}/c$, implying that waves with $k < (\hat{\omega}_{\rm pb})_{\rm e}/c$ stabilize first. The electron-driven Weibel instability should be capable of completely thermalizing the electrons. The perturbations with $k > (\hat{\omega}_{\rm pb})_{\rm e}/c$ will continue to grow even when the electron plasma is partially thermalized, with a typical value of the parameter $\eta_{\rm e} \sim 1$.

The electron beam plasma frequency, and the downstream electron plasma frequency once the electrons are fully thermalized, are similar in magnitude (see also the discussion in Wiersma & Achterberg 2004). We express them in terms of the plasma frequency $\omega_{\rm pe} = \sqrt{4\pi e^2 n_{\rm e}/m_{\rm e}}$ of the cold *upstream* electron gas with density $n_1 = n_{\rm e}$. Using the above shock relations one finds:

$$\left(\hat{\omega}_{\rm pb}\right)_{\rm e}^2 \simeq \frac{4\pi e^2 n_{\rm e}}{m_{\rm e}} = \omega_{\rm pe}^2 \;\;,\;\; \left(\tilde{\omega}_{\rm bg}\right)_{\rm e}^2 = \frac{4\pi e^2 n_2 c^2}{k_{\rm b} T_2} \simeq 12\,\omega_{\rm pe}^2. \tag{108}$$

In view of our discussion in Sect. 5.1, these estimates imply that the trapping magnetic field and the Alfvén critical field for electrons are comparable on a scale comparable to the effective skin depth: $c/\left(\tilde{\omega}_{\rm bg}\right)_{\rm e} \sim c/\left(\hat{\omega}_{\rm pb}\right)_{\rm e}$. As a result further magnetic field growth due to coalesence of the current filaments created by the electron-driven Weibel instability on a scale $r_0 \simeq c/\left(\tilde{\omega}_{\rm bg}\right)_{\rm e}$ will stall after a few mergers because of the exponential increase of the coalescence time, as calculated in Sect. A.2 of the Appendix, see also Eq. (105)). Filaments created at $r_0 \sim 1/k \ll c/\left(\tilde{\omega}_{\rm bg}\right)_{\rm e}$ will merge almost unimpeded, but the scaling laws (101) and (102) imply that the resulting magnetic field strength on a scale $r > r_0$ is comparable to the magnetic field that was created initially at that scale by the quasi-exponential phase of the Weibel instability. However, the filling factor of the current filaments decreases as merging proceeds further and further.

The ion-driven Weibel instability develops more slowly, and takes place mostly in the hot background of the already thermalized (shocked) electrons. A complication is the fact that there will possibly be strong effects in the transition layer due to electrostatic potentials generated by electron-ion charge separation, and due to a strong overshoot of the compressed magnetic field. We cannot treat these effects, but point out that -for typical parameters- magnetic effects on the Weibel instability are estimated to be small, as discussed in AW1, Sect. 8.

The ion-driven instability is weak in the sense that $\eta \ll 1$: for a hydrogen plasma one has

$$\eta_{\rm p} = \frac{\left(\hat{\omega}_{\rm pb}\right)_{\rm p}^2}{\left(\tilde{\omega}_{\rm bg}\right)_{\rm e}^2} \simeq \frac{m_{\rm e}}{m_{\rm p}} \ll 1. \tag{109}$$

The precise numerical constant in front of the electron-proton mass ratio in relation (109) is difficult to predict without a complete shock model, but will be of order unity. If one assumes charge neutrality it equals 4/3. The presence of screening currents in the hot electron background impedes the ion-driven Weibel instability for wavelengths larger than the effective electron skin depth. The screening wave number is $k_s = [(\tilde{\omega}_{\rm bg})_{\rm e}/c]\kappa_{\rm s}$, where (see AW1)

$$\kappa_{\rm s} = \begin{cases} 1 & \text{fluid background model,} \\ \left(\frac{\pi}{4}\right)^{1/3} \eta_{\rm p}^{1/6} \approx 0.26 & \text{kinetic background model.} \end{cases} \tag{110}$$

In that case relation (98) applies, the maximum trapping field in the ion-driven instability occurs at $k \sim k_{\rm s}$, and the typical field amplitude for $k > k_{\rm s}$ (up to factors of order unity) is again given by (Eq. (106)), assuming $n_{\rm p} \approx n_{\rm e} \simeq n_1$. This also implies that for protons

$$\left(\frac{v_{\rm q}}{c}\right)_{\rm p} \sim \frac{(\hat{\omega}_{\rm pb})_{\rm p}}{\sqrt{2}\,k_{\rm s} c} \leq \sqrt{\frac{\eta_{\rm p}}{2}} \simeq 0.02. \tag{111}$$

Unlike what happens with the electrons, the Weibel instability is therefore not capable of *immediately* thermalizing the incoming protons on a scale of a few times $c/(\hat{\omega}_{\rm pb})_{\rm p}$.

A second important difference with the electron-driven case is that the trapping field is smaller than the critical Alfvén field $B_{\rm A}$ for the ions on the same scale, a consequence of the larger ion mass, which makes them more difficult to deflect. One has $B_{\rm A} \sim B^{\rm tr}/\eta_{\rm p}$ at $r_0 \sim c/(\tilde{\omega}_{\rm bg})_{\rm e}$ with $\eta_{\rm p} \ll 1$. This means that merging of ion current filaments, and the associated growth of the magnetic field, is possible in principle. However, the calculations in the preceding section show that, analogous to what happens with the linear ion-driven Weibel instability at wavelengths exceeding the skin depth, further merging is impeded by the screening currents in the (now thermalized) electron background plasma. The merging rate slows down strongly once the radius of the filaments becomes larger than a few times the plasma skin depth $c/(\tilde{\omega}_{\rm bg})_{\rm e} \simeq c/(\hat{\omega}_{\rm pb})_{\rm e}$. The overal conclusion therefore is that the ion-driven Weibel instability does not generate magnetic fields that are much stronger than the ones already created by the faster electron-driven instability.

6.2. Thermalization of protons

Because the ions will thermalize well after the electrons do, the overall width of the shock transition is now determined by the ion thermalization length. To a large extent, the implications of this have already been investigated by Lyubarsky & Eichler (2006). Here we refine their calculation.

Ion thermalization takes place due to scattering in the magnetic fields that have been generated by the electron-driven Weibel instability. This process can be described as diffusion of the unit direction-of-flight vector $\hat{\boldsymbol{n}} = \boldsymbol{p}/p = (n_x,\, n_y,\, n_z)$,

where $\boldsymbol{p}$ is the proton momentum. The equation of motion for an ultra-relativistic proton with energy E can be written as

$$\frac{\mathrm{d}\hat{\boldsymbol{n}}}{\mathrm{d}s} = \frac{e}{E}\,(\hat{\boldsymbol{n}} \times \boldsymbol{B})\,. \tag{112}$$

Here s is the path length along the orbit of the proton. We neglect the influence of the shock-compressed background magnetic field as the amplitude of the Weibel-generated field is much larger: from relation (106) with $k_\mathrm{s} \sim (\tilde{\omega}_\mathrm{bg})_\mathrm{e}/c$ and (108) one finds:

$$\frac{B^\mathrm{tr}}{B_2} \approx \frac{1}{4\sqrt{3}}\left(\frac{\omega_\mathrm{pe}}{\omega_\mathrm{ce}}\right) = 4.6\times 10^2\ \sqrt{n_\mathrm{e1}}\ B_1^{-1}(\mu G). \tag{113}$$

Here $\omega_\mathrm{ce} = eB_1/m_\mathrm{e}c$ is the upstream value of the electron gyrofrequency, where we used $B_2 = 4\gamma_\mathrm{rel}\,B_\mathrm{t1} \approx 2\gamma_\mathrm{rel}\,B_1$ for the strength of the shock-compressed magnetic field. This is the limiting case of a *perpendicular shock* where the background magnetic field is along the shock surface, and is compressed most strongly.

The vector $\hat{\boldsymbol{n}}$ will diffuse with a diffusion coefficient $\mathcal{D}_{ij} \equiv \langle \Delta n_i \Delta n_j\rangle/2\Delta s$, where the angular brackets denote an ensemble average. In view of relation (113) the protons may be considered unmagnetized: the correlation length of the Weibel turbulence is much smaller than the proton gyration radius. A standard quasilinear calculation, which uses the unperturbed (ballistic) particle orbits, leads to a diffusion coefficient of the form

$$D_{ij} = \frac{\pi \mathrm{e}^2}{E^2}\int \frac{\mathrm{d}^3\boldsymbol{k}}{(2\pi)^3}\left(\hat{\boldsymbol{n}}\hat{\boldsymbol{n}} : \left\langle \tilde{\boldsymbol{A}}\tilde{\boldsymbol{A}}^*\right\rangle(\boldsymbol{k})\right)\,k_i k_j\,\delta(\boldsymbol{k}\cdot\hat{\boldsymbol{n}})\,. \tag{114}$$

The dyadic correlation tensor $\left\langle \tilde{\boldsymbol{A}}\tilde{\boldsymbol{A}}^*\right\rangle$ in this expression is the correlation tensor of the Fourier components of the vector potential $\tilde{\boldsymbol{A}}$. The Fourier components of the vector potential and of the turbulent magnetic field are related in the usual manner: $\tilde{\boldsymbol{B}} = \mathrm{i}\boldsymbol{k}\times\tilde{\boldsymbol{A}}$. The correlation tensor follows from the random phase approximation (e.g. Davidson 1972, p. 135) for the ensemble average of the turbulent fields:

$$\left\langle \tilde{\boldsymbol{A}}(\boldsymbol{k})\tilde{\boldsymbol{A}}^*(\boldsymbol{k'})\right\rangle = \left\langle \tilde{\boldsymbol{A}}\tilde{\boldsymbol{A}}^*\right\rangle(\boldsymbol{k})(2\pi)^3\,\delta^3(\boldsymbol{k}+\boldsymbol{k'})\,. \tag{115}$$

Beam protons initially have $\hat{\boldsymbol{n}} \approx \hat{\boldsymbol{z}}$. In that case the only non-vanishing components of the diffusion tensor D_{ij} are $D_{xx} = D_{yy} = D_0$, if we assume that the magnetic turbulence is axisymmetric around the beam direction. The scalar diffusion coefficient D_0 equals

$$D_0 = \frac{\pi e^2}{2E^2}\int_0^\infty \frac{\mathrm{d}k_\perp k_\perp}{(2\pi)^2}\left\langle \tilde{\boldsymbol{A}}\tilde{\boldsymbol{A}}^*\right\rangle_{zz}(k_\perp\,,\,k_\parallel=0)\,k_\perp^2\,. \tag{116}$$

Here $k_\perp = \sqrt{k_x^2+k_y^2}$ is the wave vector component perpendicular to the beam direction, and $k_\parallel = k_z$ the component along the beam direction. The trivial integration over $k_\parallel$ has been performed, using $\delta(\boldsymbol{k}\cdot\hat{\boldsymbol{n}}) = \delta(k_\parallel)$.

So far, we have considered the Weibel instability in the limit $k_\parallel = 0$. In that case the quasilinear diffusion approximation for the direction of flight $\hat{\boldsymbol{n}}$ does *not* apply, as the unperturbed orbit never leaves a single current filament. Fortunately, the assumption $k_\parallel = 0$ can be relaxed, as the Weibel instability persists for $k_\parallel \neq 0$. The theory in this case is rather complicated; see for instance the discussion in Bret et al. (2005). An approximate calculation (not reproduced here) shows that the dispersion relation for $|k_\parallel| \ll k_\perp$ leads to a dimensionless growth rate for $\kappa \ll \kappa_\mathrm{max}$ (compare Eq. (7)):

$$\sigma^2 \approx \frac{\eta\kappa^2\sin^2\theta}{\kappa_\mathrm{s}^2+\kappa^2} - 3\kappa^2\cos^2\theta. \tag{117}$$

Here $\sin\theta = k_\perp/k$, $\cos\theta = k_\parallel/k$. Formally this approximation is valid for $\eta \ll 1$, but it remains qualitatively correct for $\eta \leq 1$. The growth rate will be reduced well below the value for $\theta = \pi/2$, $\sin\theta = 1$ when $\tan^2\theta \simeq 3\,(\kappa^2+\kappa_\mathrm{s}^2)/\eta \sim 6/\eta$, where the last equality is for $\kappa \approx \kappa_\mathrm{s} \simeq 1$. For the electron-driven instability one has (at least initially) $\eta_\mathrm{e} \approx 1$, and the instability will act with a growth rate close to the maximum value for wavevectors inclined at an angle $\theta > 68$ degrees with the beam direction. This corresponds with $|\cos\theta| \leq 0.37 \equiv \cos\theta_\mathrm{c}$.

Recently, Tautz & Lerche (2007) have considered the case with $k_\parallel \neq 0$ in more detail. They show that in the asymmetric case ($\Delta \neq \frac{1}{2}$) the character of the Weibel instability changes in the sense that it is no longer aperiodic: it has $\mathrm{Re}(\omega) \neq 0$. They assume that the wave are weakly propagating, with $|\mathrm{Re}(\omega)| \ll \mathrm{Im}(\omega) = \tilde{\sigma}$, which is a good approximation for ultra-relativistic beams. We do not consider these effects here, except to point out that their (and our) analysis *excludes* the beam-resonant case where $\omega = \pm k_\parallel V_\mathrm{b} + \delta\omega$ with $|\delta\omega| \ll |k_\parallel|V_\mathrm{b}$. This case is treated by Akhiezer et al. (1975), Ch. 6.4.2.

A simple model for the turbulent power spectrum of the Weibel-generated magnetic field is

$$\begin{aligned}\left\langle|\tilde{\boldsymbol{B}}|^2\right\rangle(\boldsymbol{k}) &= k_\perp^2\,\left\langle\tilde{\boldsymbol{A}}\tilde{\boldsymbol{A}}^*\right\rangle_{zz}(k_\perp\,,\,k_\parallel)\\ &= (2\pi)^2\,\mathcal{B}(k_\perp)\,\frac{L_\parallel\,\mathrm{e}^{-k_\parallel^2 L_\parallel^2/2}}{\sqrt{2\pi}k_\perp}.\end{aligned} \tag{118}$$

Here $L_\parallel$ is the correlation length of the magnetic turbulence in the beam direction, corresponding to a bandwidth $\Delta|k_\parallel| = 1/L_\parallel$. The case $k_\parallel = 0$ corresponds with the limit $L_\parallel \longrightarrow \infty$. With this definition the rms amplitude of the turbulent magnetic field follows from:

$$\begin{aligned}B_\mathrm{rms}^2 &= \int\frac{\mathrm{d}k_\parallel\mathrm{d}k_\perp k_\perp}{(2\pi)^2}\left\langle|\tilde{\boldsymbol{B}}|^2\right\rangle(k_\perp\,,\,k_\parallel)\\ &= \int_0^\infty \mathrm{d}k_\perp\,\mathcal{B}(k_\perp).\end{aligned} \tag{119}$$

The power spectrum $\mathcal{B}(k_\perp)$ can be calculated by noting that the trapping field $B^\mathrm{tr}(k)$ (see Eq. (98)) at some wave number $k_\perp$ is related to the magnetic power spectrum $\mathcal{B}(k_\perp)$ by $\left(B^\mathrm{tr}(k\simeq k_\perp)\right)^2 \approx k_\perp\,\mathcal{B}(k_\perp)$. This yields for $k_\perp \ll k_\mathrm{max}$:

$$\mathcal{B}(k_\perp) = \frac{B_0^2}{k_\mathrm{s}}\,\frac{k_\perp/k_\mathrm{s}}{\left(1+(k_\perp/k_\mathrm{s})^2\right)^2}. \tag{120}$$

Here we define

$$B_0 = \frac{4\pi e\gamma_\mathrm{b} n_\mathrm{e}}{k_\mathrm{s}} \tag{121}$$

with n_e the density of the electron beam and $k_\mathrm{s} = \kappa_\mathrm{s}(\tilde{\omega}_\mathrm{bg})_\mathrm{e}/c$ the screening wave number. It is easy to show that this spectrum has $B_\mathrm{rms}^2 = B_0^2/2$. This spectrum falls of as $\mathcal{B}(k_\perp) \propto k_\perp^{-3}$ for $k_\perp \gg k_\mathrm{s}$, so the restriction $k_\perp < k_\mathrm{max}$ is not very important for the evaluation of integrals over the power spectrum as long as $k_\mathrm{s} \ll k_\mathrm{max}$.

Using this magnetic power spectrum in expression (116) for the scalar diffusion coefficient one finds:

$$D_0 = \frac{\sqrt{\pi} e^2 L_\parallel}{2\sqrt{2}\, E^2} \int_0^\infty \mathrm{d}k_\perp\, \mathcal{B}(k_\perp) = \frac{\sqrt{\pi}}{4\sqrt{2}} \left(\frac{eB_0}{E}\right)^2 L_\parallel. \tag{122}$$

One sees from this expression that $L_\parallel = 1/\Delta|k_\parallel|$ plays the role of a correlation length. It also shows, as argued above, that the limit $k_\parallel = 0$, $L_\parallel = \infty$ is formally ill-defined.

If we define a gyroradius $r_\mathrm{g} = E/eB_0$ one has:

$$D_0 = \frac{\sqrt{\pi}}{4\sqrt{2}} \frac{L_\parallel}{r_\mathrm{g}^2}\cdot \tag{123}$$

Lyubarsky & Eichler (2006) arrive at a similar expression, in effect putting $L_\parallel \sim 1/k_\mathrm{s}$ and neglecting the numerical constant. In view of our discussion above of the behavior of the Weibel instability for $\theta < \pi/2$ the obvious choice for $L_\parallel$ is

$$L_\parallel \sim \frac{1}{k_\mathrm{s} \cos\theta_\mathrm{c}} \approx \frac{2.65}{k_\mathrm{s}}\cdot \tag{124}$$

Here we use the fact that the largest contribution to the integral over the power spectrum comes from the region $k_\perp \simeq k_\mathrm{s}$. This gives

$$D_0 = 0.83 \left(\frac{r_\mathrm{sk}}{r_\mathrm{g}^2}\right), \tag{125}$$

with $r_\mathrm{sk} = 1/k_\mathrm{s}$ the effective skin depth of the hot electron background, which according to (108) equals

$$r_\mathrm{sk} \simeq \frac{c}{(\tilde{\omega}_\mathrm{bg})_\mathrm{e}} = \frac{1}{2\sqrt{3}} \frac{c}{\omega_\mathrm{pe}}\cdot \tag{126}$$

As protons are scattered by the random fields the components of the direction of flight satisfy (cf. Achterberg et al. 2003)

$$\left\langle n_x^2 \right\rangle = \left\langle n_y^2 \right\rangle \approx 2\mathcal{D}_0 s \;\;,\;\; \left\langle n_z^2 \right\rangle \approx 1 - 4\mathcal{D}_0 s, \tag{127}$$

where the brackets indicate an average over the distribution. This shows that the thermalization length is

$$\ell_\mathrm{th} = \frac{1}{6\mathcal{D}_0} \simeq 0.2 \left(\frac{r_\mathrm{g}^2(E)}{r_\mathrm{sk}}\right), \tag{128}$$

the distance where according to (127) one has $\left\langle n_x^2 \right\rangle = \left\langle n_y^2 \right\rangle = \left\langle n_z^2 \right\rangle = 1/3$, corresponding to an isotropic distribution of momenta. The more precise theory in Achterberg et al. (2003) shows that ℓ_th is indeed the relevant length scale: the initial correlation of the momentum directions of the beam particles decays due to scattering as $\exp(-6D_0 s)$ with distance s.

Using (121) with $k_\mathrm{s} \simeq (\tilde{\omega}_\mathrm{bg})_\mathrm{e}/c \simeq 2\sqrt{3}\,\omega_\mathrm{pe}/c$ (as $\kappa_\mathrm{s} \simeq 1$ in the electron-driven instability) one has for beam protons with energy $E \simeq \gamma_\mathrm{b} m_\mathrm{p} c^2$:

$$r_\mathrm{g} \simeq \frac{m_\mathrm{p} c^2 k_\mathrm{s}}{4\pi e^2 n_\mathrm{p}} = \frac{c\,(\tilde{\omega}_\mathrm{bg})_\mathrm{e}}{(\hat{\omega}_\mathrm{pb})_\mathrm{p}^2} \simeq 2\sqrt{3} \left(\frac{m_\mathrm{p}}{m_\mathrm{e}}\right) \frac{c}{\omega_\mathrm{pe}}\cdot \tag{129}$$

Here n_p is the density of beam protons, which equals n_e beacause of quasi-neutrality in the upstream flow, and we have used relation (108). This gives the proton thermalization length in terms of the upstream electron skin depth c/ω_pe:

$$\ell_\mathrm{th}^\mathrm{p} = 8.3 \left(\frac{m_\mathrm{p}}{m_\mathrm{e}}\right)^2 \frac{c}{\omega_\mathrm{pe}} \simeq 1.5 \times 10^{13} n_\mathrm{e}^{-1/2}\ \mathrm{cm}. \tag{130}$$

Apart from the numerical factor ~8, this is the same result as derived by Lyubarsky & Eichler (2006).

7. Conclusions

In this paper we have presented two detailed nonlinear calculations of the saturation of the Weibel instability driven by ultra-relativistic beams. The first uses a relativistic fluid approximation to calculate the response of the beam particles, while the second uses kinetic plasma theory for the beam plasma. Although the physics of the two calculations is subtly different, pertaining respectively to the case of a single dominant mode where wave breaking occurs and to fake diffusion in a broad-band collection of waves due to the quiver motion that "heats" the beam plasma in the plane perpendicular to the beam direction, these calculations both confirm that the Weibel instability due to relativistic beams will end the phase of exponential growth when particle trapping occurs, i.e. when the amplitude of the quiver motion, driven by the Lorentz force of the wave-generated magnetic field, becomes comparable with the wavelength of the unstable modes. A similar conclusion was reached by Davidson et al. (1972) for the Weibel instability in a non-relativistic plasma with a temperature anisotropy, by Yang et al. (1994) for the Weibel instability in a magnetized electron-positron plasma, and our results also confirm the estimate of Gruzinov (2001) (see also: Wiersma & Achterberg 2004) for this particular case. This means that the typical field strength at the end of the quasi-exponential phase of the instability is independent of the mass of the beam particles in a hydrogen plasma. The fast electron-driven Weibel instability creates a field that is approximately two orders of magnitude larger than the shock-compressed magnetic field, see Eq. (113). Its value is set by the skin depth (inertial length) c/ω_pe and density of the upstream electron plasma, $B \sim \pi e n_\mathrm{e}(c/\omega_\mathrm{pe})$, *independent* of the shock Lorentz factor. The slower proton-driven instability is impeded by the presence of the now thermalized post-shock electron gas. The trapping argument shows that the typical field strength associated with this instability is of the same order as the field generated by the electron-driven instability: once the rapidly growing electron-driven instability has stabilized and the electron beams have thermalized, the electron screening currents result in a the trapping field that is independent of the mass of the beam particles driving the instability.

We have also considered the subsequent development of the magnetic fields generated by the Weibel instability. We point out that the merging of current filaments (as proposed by Medvedev et al. 2005) and the associated algebraic growth of the magnetic field associated with these filaments, is slowed down drastically by the effects of screening currents once the the transverse size of the filaments and the filament-filament separation distance becomes comparable with, or larger than with the electron skin depth. The coalescence time increases exponentially as the merged filaments are further and further apart. This limits any further field amplification (or decay) on scales larger than the skin depth. On smaller scales, the merging is essentially unimpeded, but the resulting magnetic field on some scale r has an amplitude comparable to the trapping field left behind by the Weibel instability at that scale. Therefore, the magnetic field strength never grows much beyond the trapping field.

Other models of filament evolution (e.g. Kato 2005) stress the fact that particle orbits inside filaments become chaotic once the Alfvén limit is reached. This would lead to thermalization of the beam kinetic energy. Our calculations indicate that this is indeed the case for the electron-driven instability, leading to rapid thermalization of the electron beams, but will almost certainly never happen for the much heavier ions. Screening currents in the already thermalized electron plasma prevent the magnetic

field from rapidly growing to a strength that corresponds to the Alfvén limit for ions.

We have used our estimates for the post-shok magnetic field created by the electron beams to calculate the effect of the magnetic turbulence on the ion beams that, in contrast to what happens to the electrons, are not *directly* thermalized by the Weibel instability. Ion thermalization happens indirectly, not through phase-mixing of the quiver motion, but by the slow scattering on the turbulent magnetic fields left by the Weibel instability. Our calculation of the thermalization length confirms the basic idea of Lyubarsky & Eichler (2006), albeit with a thermalization length that is one order of magnitude larger than their value.

We have not adressed in this paper the *long-term* survival of these filamentary magnetic fields in the post-shock flow. Recent numerical simulations for relativistic shocks in an electron-positron plasma (Chang et al. 2007) with a sufficiently large simulation box indicate that the magnetic field decays as $B \sim t^{-1}$ sufficiently far (hundreds of skin depths) behind the shock. The $B(t) \propto t^{-1}$ behavior was predicted by Gruzinov (2001).

Appendix A: The coalescence of partially screened current filaments

The hot background plasma that one expects to be present in shock transition layers will influence the coalescence process because it supports screening currents, which diminish both the total current associated with a filament, and the resulting magnetic field outside the filament. The latter determines the strength of the force between adjacent current filaments. In this section we give an approximate calculation of the influence of screening currents on the merger rate, and show how this modifies the results of the simple merger model employed above for $r_m > c/\tilde{\omega}_{\rm bg}$.

The magnitude of the screening current in the z-direction (along the beams) that is carried by the background can be readily calculated from the z-component of the equation of motion for species s in the hot background. This equation is formally identical to the corresponding Eq. (29) for the beam particles. The only difference is that the effective inertia of a hot plasma is $m_{\rm s}h_{\rm s}$ with $h_{\rm s}$ the enthalpy per unit rest energy, cf. Landau & Lifschitz (1959). One has:

$$m_{\rm s}h_{\rm s}\,\frac{{\rm d}\,(\gamma_{\rm s}V_{{\rm s}z})}{{\rm d}t} = q_{\rm s}\left(\boldsymbol{E}+\frac{\boldsymbol{V}\times\boldsymbol{B}}{c}\right)_z. \tag{A.1}$$

In a cylindrically symmetric situation around a straight filament where the axis coincides with the z-axis, with $\boldsymbol{B} = B(r)\,\hat{\boldsymbol{\phi}}$ and $\partial/\partial\phi = 0$, one has $B(r) = -\partial A/\partial r$, $(\boldsymbol{V}\times\boldsymbol{B})_z = V_r B(r)$, $E_z = -(1/c)(\partial A/\partial t)$ and ${\rm d}/{\rm d}t = \partial/\partial t + V_r\,(\partial/\partial r)$. Here $\boldsymbol{A} = A(r)\,\hat{\boldsymbol{z}}$ is the vector potential, r is the cylindrical radius centered on the filament axis and ϕ is the azimuthal angle around the filament. In that case Eq. (A.1) can be integrated to

$$m_{\rm s}h_{\rm s}\gamma_{\rm s}V_{{\rm s}z} + \frac{q_{\rm s}A}{c} = \text{constant} \equiv \mathcal{P}_{{\rm s}z}, \tag{A.2}$$

which is the equivalent of relation (33) for a species belonging to the background plasma. For a growing field the integration constant $\mathcal{P}_{{\rm s}z}$ can be neglected. Solving for $V_{{\rm s}z}$ with $\mathcal{P}_{{\rm s}z} = 0$ one finds the screening current due to the background:

$$\begin{aligned}\boldsymbol{J}_{\rm bg} &= \sum_{\rm s} q_{\rm s}n_{\rm s}V_{{\rm s}z}\,\hat{\boldsymbol{z}}\\ &= -\sum_{\rm s}\frac{q_{\rm s}^2 n_{\rm s}}{m_{\rm s}h_{\rm s}c}\,\frac{\boldsymbol{A}}{\sqrt{1+\left(\dfrac{q_{\rm s}A}{m_{\rm s}h_{\rm s}c^2}\right)^2}}.\end{aligned} \tag{A.3}$$

In what follows we will neglect the nonlinearity in this relation due to the relativistic mass correction, replacing (A.3) by its non-relativistic equivalent

$$\boldsymbol{J}_{\rm bg} \approx -\sum_{\rm s}\frac{q_{\rm s}^2 n_{\rm s}}{m_{\rm s}h_{\rm s}c}\,\boldsymbol{A} = -\frac{\tilde{\omega}_{\rm bg}^2}{4\pi c}\,\boldsymbol{A}. \tag{A.4}$$

This is allowed if $J_{\rm s} \ll n_{\rm s}q_{\rm s}c$, which is formally satisfied if the beam density satisfies $\overline{n}_{\rm b} \ll n_{\rm s}$, or if the beam-current filaments have a size $r_0 \ll c/\tilde{\omega}_{\rm bg}$ so that the screening currents remain small. For the fields created by the Weibel instability this last condition is (marginally) satisfied. Nevertheless, our results should remain *qualitatively* valid even when $J_{\rm s} \approx n_{\rm s}q_{\rm s}c$.

We note in passing that relation (A.3) implies that $J_{\rm s} < n_{\rm s}q_{\rm s}c$, a limit which is physically obvious. Therefore, in a situation where the beam density is much larger than the density of the species in the background plasma so that $\overline{n}_{\rm b} \gg n_{\rm s}$ for all species, screening currents are always much smaller than the maximum current density that can be carried by the beam, $J_{\rm b} = \overline{n}_{\rm b}q_{\rm b}c$. In that case screening can be much less effective. In what follows we will assume that (at most) $\overline{n}_{\rm b} \approx n_{\rm s}$, and that this particular situation does not occur.

In a quasi-steady state, where the fields only depend on the distance r from the filament axis and $\boldsymbol{A} = A(r)\,\hat{\boldsymbol{z}}$, Maxwell's equation for the vector potential $\boldsymbol{\nabla}\times(\boldsymbol{\nabla}\times\boldsymbol{A}) = (4\pi/c)\,\boldsymbol{J}$ (e.g. Jackson 1975, Ch. 6.4) reads, with approximation (A.4),

$$\frac{1}{r}\,\frac{\partial}{\partial r}\left(r\,\frac{\partial A}{\partial r}\right) - \frac{\tilde{\omega}_{\rm bg}^2}{c^2}\,A = -\frac{4\pi}{c}\,J_{\rm b}. \tag{A.5}$$

Here $J_{\rm b}$ is the current density due to the beam particles in a current filament. The screening current of the background plasma corresponds to the second term on the lefthand side of the equation.

Let us calculate the magnetic field due to a single cylindrical current filament embedded in a background plasma with a uniform background density $n_{\rm s}$ and pressure $P_{\rm s}$. This last assumption is a reasonable approximation as long as the radial gradients in pressure and density induced by the radial magnetic pinching force remain small. This will be the case if $B^2/8\pi \ll P_{\rm s}$. In the relativistic case this condition is met when the field amplitude is much less than the equipartition field: $B \ll B_{\rm e}$. As a first approximation, the current density carried by the beam is taken to be constant over the cross section of the filament of radius r_0, $J_{\rm b} = J_0$ for $r \le r_0$, and vanishes outside the filament: $J_{\rm b} = 0$ for $r > r_0$.

Equation (A.5) is readily solved for constant $\tilde{\omega}_{\rm bg}$ in terms of the modified Bessel functions of integer order, $I_{\rm n}$ and $K_{\rm n}$:

$$A(r) = \frac{4\pi J_0}{ck_{\rm s}^2} \times \begin{cases} 1 - k_{\rm s}r_0\, K_1(k_{\rm s}r_0) I_0(k_{\rm s}r) & \text{for } r \le r_0; \\ \\ k_{\rm s}r_0\, I_1(k_{\rm s}r_0) K_0(k_{\rm s}r) & \text{for } r > r_0. \end{cases} \tag{A.6}$$

Here $k_{\rm s} \equiv \tilde{\omega}_{\rm bg}/c$ is the inverse skin depth. The magnetic field as a function of cylindrical radius r follows from $B(r) = -\partial A/\partial r$:

$$B(r) = 2B_0 \times \begin{cases} K_1(k_{\rm s}r_0) I_1(k_{\rm s}r) & \text{for } r \le r_0; \\ \\ I_1(k_{\rm s}r_0) K_1(k_{\rm s}r) & \text{for } r > r_0. \end{cases} \tag{A.7}$$

Here $B_0 = 2\mathcal{I}_0/cr_0 = 2\pi r_0 J_0/c$ is the field at the outer radius r_0 of an unscreened current filament with a total beam current $\mathcal{I}_0 = \pi r_0^2\, J_0$. The *total* current contained within a cylindrical radius r_0 equals

$$\mathcal{I}_{\rm tot} = \frac{cr_0\, B(r_0)}{2} = 2\mathcal{I}_0\, I_1(k_{\rm s}r_0) K_1(k_{\rm s}r_0). \tag{A.8}$$

For a large current filament, with a radius such that $k_{\rm s}r_0 \gg 1$, $\mathcal{I}_{\rm tot}$ decays with increasing filament radius as

$$\mathcal{I}_{\rm tot} \approx \mathcal{I}_0/k_{\rm s}r_0, \tag{A.9}$$

while the magnetic field for $r > r_0$ falls off rapidly:

$$B(r) \approx B_0\, \frac{{\rm e}^{-k_{\rm s}(r-r_0)}}{k_{\rm s}\sqrt{rr_0}}. \tag{A.10}$$

A.1. Equation of motion for two attracting screened filaments

Now consider two identical, straight and parallel current filaments of radius r_0, with their axes parallel to the z-axis at a distance $d > 2r_0$. This is the situation at the end of the Weibel instability with $k_z = 0$ that we have described in the previous sections, where the instability has led to a filamentary distribution of currents. This is the situation seen in various numerical simulations.

As an admittedly crude model let us assume that we can describe the interaction between the two current filaments as the interaction between two current wires, with a total current equal to the partially screened current $\mathcal{I}_{\rm tot}$ of Eq. (A.8), and with a magnetic field outside the filament given by Eq. (A.7). The attractive interaction force per unit length between the current wires equals ${\rm d}F/{\rm d}\ell = -\mathcal{I}_{\rm tot}B(d)/c$, which is

$$\frac{{\rm d}F}{{\rm d}\ell} = -\frac{8\mathcal{I}_0^2}{c^2 r_0}\, I_1^2(k_{\rm s}r_0) K_1(k_{\rm s}r_0) K_1(k_{\rm s}d). \tag{A.11}$$

For $k_{\rm s}r_0 \ll 1$ and $k_{\rm s}d \ll 1$ we can use the expansion of the modified Bessel functions for a small argument: $I_1(\xi) \approx \xi/2$ and $K_1(\xi) \approx 1/\xi$. In that case (A.11) reduces to the well-known result ${\rm d}F/{\rm d}\ell = -2\mathcal{I}_0^2/c^2 d$.

The mass per unit length of a current filament is approximately equal to

$$\mu \equiv \frac{{\rm d}m}{{\rm d}\ell} \approx \pi r_0^2\, (n_{\rm e}m_{\rm e}h_{\rm e} + \gamma_{\rm b}m_{\rm b}\overline{n}_{\rm b})\,. \tag{A.12}$$

Here we have used that the effective mass of the hot electron background equals $m_{\rm eff} \approx m_{\rm e}h_{\rm e}$, and that the effective mass of the beam particles for motions perpendicular to the beam direction is $\gamma_{\rm b}m_{\rm b}$. This assumes that the beam currents and the hot electron background, which provides the screening current, move together inside the filament.

The equation of motion for a filament is

$$\mu\, \frac{{\rm d}^2 d}{{\rm d}t^2} = -\frac{8\mathcal{I}_0^2}{c^2 r_0}\, I_1^2(k_{\rm s}r_0) K_1(k_{\rm s}r_0) K_1(k_{\rm s}d). \tag{A.13}$$

The modified Bessel function K_0 satisfies ${\rm d}K_0(\xi)/{\rm d}\xi = -K_1(\xi)$. This means that the force on the righthand side of Eq. (A.13) can be written as $-\partial V_{\rm int}/\partial d$, where the interaction potential $V_{\rm int}(d)$ is given by:

$$V_{\rm int}(d) = -\frac{8\mathcal{I}_0^2}{k_{\rm s}c^2 r_0}\, I_1^2(k_{\rm s}r_0) K_1(k_{\rm s}r_0) K_0(k_{\rm s}d). \tag{A.14}$$

A.2. The coalescence time scale

If the filaments start from rest at an initial distance $d_{\rm i}$, the equation of motion has an energy integral:

$$\frac{\mu}{2}\left(\frac{{\rm d}d}{{\rm d}t}\right)^2 + V_{\rm int}(d) = V_{\rm int}(d_{\rm i}). \tag{A.15}$$

The coalescence time now follows as

$$t_{\rm coal}(d_{\rm i}) = \int_{2r_0}^{d_{\rm i}} \frac{{\rm d}r}{\sqrt{\dfrac{2}{\mu}\,[V_{\rm int}(d_{\rm i}) - V_{\rm int}(r)\,]}}. \tag{A.16}$$

Here we end the coalescence phase when the filaments touch so that $d = 2r_0$. Defining dimensionless variables,

$$\varpi \equiv k_{\rm s}d \;\;,\;\; \varpi_0 \equiv k_{\rm s}r_0, \tag{A.17}$$

one finds

$$t_{\rm coal}(\varpi_{\rm i}) = T_0 \int_{2\varpi_0}^{\varpi_{\rm i}} \frac{{\rm d}\varpi}{\sqrt{K_0(\varpi) - K_0(\varpi_{\rm i})}}, \tag{A.18}$$

with a characteristic time T_0 given by

$$\begin{aligned} T_0 \;&\equiv \left(\frac{16\mathcal{I}_0^2 k_{\rm s}}{\mu c^2\, r_0}\right)^{-1/2} \left(I_1^2(\varpi_0)K_1(\varpi_0)\right)^{1/2} \\ &= \frac{1}{2\hat{\omega}_{\rm pb}} \left(\frac{c}{V_{\rm b}}\right) \left(1 + \frac{n_{\rm e}m_{\rm e}h_{\rm e}}{\overline{n}_{\rm b}m_{\rm b}\gamma_{\rm b}}\right)^{1/2} \left(\frac{B_0}{B_{\rm b}}\right)^{-1} \psi(\varpi_0). \end{aligned} \tag{A.19}$$

Here we define

$$\psi(\varpi_0) \equiv 1/\sqrt{\varpi_0\, I_1^2(\varpi_0)K_1(\varpi_0)}, \tag{A.20}$$

normalize the beam current with the maximum current $I_{\rm b} = \pi r_0^2 q_{\rm b}\overline{n}_{\rm b}c$ and use $\mathcal{I}_0/\mathcal{I}_{\rm b} = B_0/B_{\rm b}$. Note that for current filaments left by the Weibel instability the trapping argument predicts that $B_0 \approx B_{\rm b}$ and that $V_{\rm b} \simeq c$ for the relativistic beams we are considering. In that case (for typical values of the parameters) one has $T_0 \simeq 1/\hat{\omega}_{\rm pb}$ for $r_0 \sim c/\tilde{\omega}_{\rm bg}$, and the time scale of the merging process and the growth time of the preceding Weibel instability, $t_{\rm W} \sim 1/\tilde{\sigma} \simeq 1/\hat{\omega}_{\rm pb}$, are of the same order.

In what follows we will neglect the factor $\sqrt{1+n_\mathrm{e}m_\mathrm{e}h_\mathrm{e}/\overline{n}_\mathrm{b}\gamma_\mathrm{b}m_\mathrm{b}}$, which is always of order unity in our applications. Assuming $\varpi_0 \gg 1$ and $\varpi_i \gg 1$ we can use the asymptotic expansion of the modified Bessel functions for large arguments, $I_\mathrm{n}(\varpi) \approx \mathrm{e}^{\varpi}/\sqrt{2\pi\varpi}$ and $K_\mathrm{n}(\varpi) \approx \sqrt{\pi/2\varpi}\,\mathrm{e}^{-\varpi}$. In that case

$$\psi(\varpi_0) \approx (8\pi\varpi_0)^{1/4}\,\mathrm{e}^{-\varpi_0/2}, \tag{A.21}$$

and the integral appearing in (A.18) can be approximated by

$$\left(\frac{2}{\pi}\right)^{1/4}\int_{2\varpi_0}^{\varpi_\mathrm{i}}\frac{\mathrm{d}\varpi\,\varpi^{1/4}\,\mathrm{e}^{\varpi/2}}{\sqrt{1-(\varpi/\varpi_\mathrm{i})^{1/2}\,\mathrm{e}^{\varpi-\varpi_\mathrm{i}}}} \equiv \mathcal{K}. \tag{A.22}$$

In its present form the integral cannot be evaluated analytically. However, for $2\varpi_0 \gg 1$ an excellent approximation can be derived. To that end we define a new variable,

$$\zeta \equiv \left(\frac{\varpi}{\varpi_\mathrm{i}}\right)^{1/4}\mathrm{e}^{(\varpi-\varpi_\mathrm{i})/2}. \tag{A.23}$$

With a little algebra it is easy to show that the integral (A.22) can be rewritten as

$$\mathcal{K} = 2\left(\frac{2\varpi_\mathrm{i}}{\pi}\right)^{1/4}\mathrm{e}^{\varpi_i/2}\int_{\zeta_0}^{1}\frac{\mathrm{d}\zeta}{\sqrt{1-\zeta^2}\;[\,1+1/2\varpi(\zeta)\,]}. \tag{A.24}$$

For $\varpi \gg 1$ we can safely neglect $1/2\varpi$ in the factor $(1+1/2\varpi)$, and the integral becomes

$$\mathcal{K} \approx 2\left(\frac{2\varpi_\mathrm{i}}{\pi}\right)^{1/4}\mathrm{e}^{\varpi_i/2}\left(\frac{\pi}{2}-\sin^{-1}(\zeta_0)\right). \tag{A.25}$$

Together with (A.18), (A.19) and (A.21) this gives the coalescence time for $\zeta_0 = (2\varpi_0/\varpi_\mathrm{i})^{1/4}\exp[(2\varpi_0-\varpi_\mathrm{i})/2\,] \ll 1$:

$$t_\mathrm{coal} \approx \frac{2\pi}{\hat{\omega}_\mathrm{pb}}\left(\frac{B_0}{B_\mathrm{b}}\right)^{-1}\left(\frac{c}{V_\mathrm{b}}\right)(\varpi_0\varpi_\mathrm{i})^{1/4}\;\mathrm{e}^{(\varpi_\mathrm{i}-2\varpi_0)/2}. \tag{A.26}$$

For $\varpi_\mathrm{i}-\varpi_0 \geq \varpi_0 \gg 1$ the coalescence time grows exponentially with increasing distance between the two filaments.

References

Achterberg, A., & Wiersma, J. 2007, A&A, 475, 1
Achterberg, A., Gallant, Y. A., Rachen, J. P., Norman, C. A., & Melrose, D. B. 2003, MNRAS, submitted
Akhiezer, A. I., Akhiezer, I. A., Polovin, R. V., Sitenko, A. G., & Stepanov, K. N. 1975, Plasma Electrodynamics Vol. 1: Linear Theory (Oxford: Pergamon Press)
Blandford, R. D., & McKee, C. F. 1976, Phys. Fluids, 19, 1130
Bret, A., Firpo, M.-C., & Deutsch, C. 2005, Laser and Particle Beams, 23, 375
Cary, J. R., & Kaufman, A. N. 1981, Phys. Fluids, 24, 1238
Chang, P., Spitkovsky, A., & Arons, J. A. 2007 [arXiv:astro-ph 0704.3832]
Davidson, R. C. 1972, Methods in Nonlinear Plasma Theory (New York: Academic Press)
Davidson, R. C., Hammer, D. A., Haber, I., & Wagner, C. E. 1972, Phys. Fluids, 15, 317
Frederiksen, J. T., Hededal, C. B., Haugbølle, T., & Nordlund, Å. 2004, ApJ, 608, L13
Galeev, A. A., & Sagdeev, R. S. 1979, in Reviews of Plasma Physics, ed. M. A. Leontovich (New York: Consultants Bureau), 7, 1
Gruzinov, A. 2001, ApJ, 563, L15
Ichimaru, S. 1973, Basic Principles of Plasma Physics (USA: W.A. Benjamin Inc., Reading, Ma.)
Jackson, J. D. 1975, Classical Electrodynamics, 2nd edn. (New York: John Wiley & Sons)
Kadomtsev, B. B. 1965, Plasma Turbulence (London: Academic Press)
Kato, T. N. 2005, Phys. Plasmas, 12, 080705
Landau, L. D., & Lifschitz, E. M. 1959, Fluid Mechanics (Oxford: Pergamon Press)
Lee, R., & Lampe, M. 1973, Phys. Rev. Lett., 31, 1390
Lyubarsky, & Eichler 2006, ApJ, 647, 1250
Medvedev, M. V. 2000, ApJ, 540, 704
Medvedev, M. V., & Loeb, A. 1999, ApJ, 526, 697
Medvedev, M. V., Fiore, M., Fonseca, R. A., Silva, L. O., & Mori, W. B. 2005, ApJ, 618, L75
Melrose, D. B. 1986, Instabilities in Space and Laboratory Plasmas (Cambridge University Press)
Mészáros, P. 2002, ARA&A, 40, 137
Mészáros, P. 2006, Rep. Prog. Phys., 69, 2259
Milosavljević, M., & Nakar, E. 2006, ApJ, 641, 978
Piran, T. 2000, Phys. Rep., 333, 529
Piran, T. 2004, Rev. Mod. Phys., 76, 1143
Rees, M. J., & Mészáros, P. 1992, MNRAS, 258, 41
Rees, M. J., & Mészáros, P. 1994, ApJ, 430, L93
Roberts, P. H. 1967, An Introduction to Magnetohydrodynamics (London: Longmans, Green and Co. Ltd)
Tautz, R. C., & Lerche, I. 2007, Phys. Plasmas, 14, 072102
Wiersma, J., & Achterberg, A. 2004, A&A, 428, 365
Wijers, R. A. M. J., & Galama, T. J. 1999, ApJ, 523, 177
Yang, T.-Y. B., Arons, J., & Langdon, A. B. 1994, Phys. Plasmas, 1, 3059